This article has been accepted for publication in IEEE Transactions on Automatic Control. This is the author's version which has not been fully edited and content may change prior to final publication. Citation information: DOI 10.1109/TAC.2023.3342060

Analysis of H_∞ Performance for Multi-Agent Networks

Jiamin Wang, Jian Liu, Yuanshi Zheng, *Senior Member, IEEE*, and Jianxiang Xi

***Abstract*— In this paper, we analyze the H_∞ performance of the first-order continuous-time multi-agent consensus network and that of the corresponding sampled-data network in the presence of external disturbances. Firstly, we build the quantitative relation between the H_∞ performance and the eigenvalues of directed graph Laplacian for the continuous-time multi-agent network. Secondly, we establish the analytic expression of H_∞ performance for the sampled-data multi-agent network, which depends not only the eigenvalues of Laplacian matrix but also the sampling period. It is proved that there exists a unique optimal sampling period such that the sampled-data multi-agent network obtains the optimal H_∞ performance. Furthermore, we show that the H_∞ performance of the sampled-data multi-agent network is not better than that of the original continuous-time multi-agent network. Finally, numerical tests are given on several well-known graphs.**

***Index Terms*— Consensus networks, H_∞ performance, graph Laplacian, optimal sampling period**

I. Introduction

THE consensus problem of multi-agent networks has been extensively investigated in control community for decades since Jadbabaie et al. [1] provided a theoretical explanation for the Vicsek model [2] that characterizes the coordination behaviors of a group of autonomous agents. Generally speaking, consensus means that agents in a network reach an agreement regarding a common quantity of interest [3] such as opinions, positions, velocities, and directions, by designing an appropriate local interaction rule. A common line of investigation is to examine the consensus on various dynamic models of agents such as first-order, second-order, continuous-time, and discrete-time multi-agent networks. Some results have been reported in [1], [3], [4]. Furthermore, research on consensus problems in heterogeneous [5], [6] and hybrid [7]–[10] multi-agent networks enriches the theoretical results and expands the field of consensus problems.

This work was funded by the National Natural Science Foundation of China (62273267), the Natural Science Basic Research Program of Shaanxi, China (2022JC-46, 2023-JC-YB-525 and 2023-JC-QN-0766), and the Fundamental Research Funds for the Central Universities, China (ZYTS23021). The material in this paper was not presented at any conference. *(Corresponding author: Yuanshi Zheng)*

Jiamin Wang, Jian Liu and Yuanshi Zheng are with Shaanxi Key Laboratory of Space Solar Power Station System, School of Mechano-electronic Engineering, Xidian University, Xi'an, 710071, China (E-mail: wangjiamin21@outlook.com; liujianzym@outlook.com; zhengyuanshi2005@163.com).

Jianxiang Xi is with Rocket Force University of Engineering, Xi'an, 710025, China (E-mail: xijx07@mails.tsinghua.edu.cn).

Another topic that is closely related to consensus is the robustness of multi-agent networks against uncertainties. The uncertainties, such as external disturbances, measurement noises, communication time-delays, and model uncertainties, are rife in reality, which may cause agents to deviate from consensus and deteriorate some expected performance. Typically, the robustness of consensus networks to external disturbances is measured by H_2 norm or H_∞ norm, which is also termed H_2 performance or H_∞ performance. Some studies involved the relation between H_2 performance and network topology [11]–[13]. In [11], the authors characterized the robustness of consensus networks against white noise as the H_2 norm of the closed-loop system, which depends on the eigenvalues of graph Laplacian. Similarly, further results for second-order node dynamics and time-delay were, respectively, explored in [12] and [13]. There are growing works for H_∞ performance. Most of them concentrated on the H_∞ consensus based on robust control theory with linear matrix inequality (LMI) [14]–[19]. In [14], the authors took model uncertainties, time-delays, and external disturbances into consideration and solved the H_∞ consensus problem with a given H_∞ performance index by using the LMI technique. Then the authors in [15] proposed a necessary and sufficient condition for the H_∞ output consensus problem of multi-agent networks with higher-order integrator dynamics by model transformation and H_∞ control theory. Subsequently, they extended the results to multi-agent networks with general linear dynamics [16]. Besides, the concept of H_∞ performance region to analyze the existence of distributed controller was introduced in [17]. The mixed H_2/H_∞ consensus problem was solved in [18] via an inner auxiliary system approach. Recently, authors in [19] solved the H_∞ bipartite tracking consensus problem for multi-agent networks with nonlinear dynamics over directed signed graphs in the presence of external disturbances. It should be noted that the analysis methods of H_∞ performance in the above works are based on LMIs. However, they did not reveal the quantitative relation between the H_∞ performance and the topological structure of the network.

A few studies investigated the relation between H_∞ performance and network topology [20]–[24]. For undirected graphs, it was showed in [20] that the H_∞ performance is determined by the minimum eigenvalue of the grounded Laplacian matrix of the first-order leader-follower multi-agent system. In [21], the authors built the relation between the H_∞ performance of the first-order linear consensus network and the minimum non-zero eigenvalue of Laplacian matrix of the undirected graph. Authors in [22] investigated the first-order linear multi-agent network with edge consensus protocol on the unweighted undirected graph, and obtained the expressions of H_∞ performance by using the similarity transformation based on the incidence matrix and the edge Laplacian. Recently, a concise graph condition was proposed in [23] for second-order multi-agent systems to tell which one of the absolute and relative velocity protocols has a better anti-disturbance capability. For directed graphs, it was shown in [24] that the H_∞ performance of first-order leader-follower multi-agent system depends on the minimum singular value of the grounded Laplacian matrix. Note that authors in [20] and [24] considered the special multi-agent system, i.e., the leader-follower multi-agent system, whose subsystem formed by followers is a positive system. Therefore, the maximum singular values in H_∞ norms of transfer matrices occurred at zero frequency. Moreover, the analysis in [22] also relied on the zero frequency. Unfortunately, this property is invalid for the classic first-order multi-agent consensus network on the weighted directed graph. In addition, there are some limitations in existing works. On the one hand, the expressions of H_∞ performance in [22] derived on unweighted undirected graphs are implicit. Thus, they are not conducive to design consensus network against disturbances. It may be difficult to build explicit expressions of H_∞ performance on weighted directed graphs by using their method. On the other hand, H_∞ performance in the all above literature characterized the influence of uncertainties only on consensus. By contrast, authors in [25] provided the optimal network topology in the absence of external disturbances by minimizing a quadratic performance index which included disagreement energy and control effort. Inspired by the above observations, we intend to further study the H_∞ performance from disturbance to consensus and control effort for first-order continuous-time multi-agent consensus network, build quantitative relation between the H_∞ performance and the weighted directed network topology, and explore the consensus network with the optimal H_∞ performance.

Note that the above works all paid attention to the robustness of continuous-time multi-agent networks. However, interactions among agents are usually implemented by digital sensors and controllers which only permit information transmission in the form of sampling data in engineering manipulation. Therefore, sampling control for continuous-time multi-agent networks is particularly valuable in applications, which has received much interest (see [26]–[28] and survey paper [29] for more details). Following from the above facts, some questions naturally arise: 1) *Whether there exists the optimal sampling period in the presence of disturbances*? 2) *Does sampling control deteriorate or improve the H_∞ performance*? The problems raised above inspire us to further study the quantitative relation between H_∞ performance, network topology, and sampling period for sampled-data multi-agent consensus networks, and reveal the relation between the H_∞ performance of continuous-time and that of corresponding sampled-data multi-agent networks.

In this paper, we first investigate the quantitative relation between the H_∞ performance and the network topology for continuous-time multi-agent consensus networks. Then, we analyze the existence of optimal sampling period for sampled-data multi-agent consensus networks. Moreover, the relation between the H_∞ performance of continuous-time multi-agent networks and the H_∞ performance of corresponding sampled-data networks is studied. The main contributions of this paper can be summarized as follows:

1. Different from existing works, the H_∞ performance in this paper concerns the influence of disturbances on consensus and control effort together. We build quantitative relation between the H_∞ performance of the first-order continuous-time multi-agent network and the eigenvalues of Laplacian matrix associated with the weighted directed graph by orthogonal transformation technique. For the weighted undirected graph, we derive quantitative relation between the H_∞ performance and the minimum non-zero eigenvalues of Laplacian matrix. It facilitates designing the optimal consensus network against disturbances.

2. We establish quantitative relation between the H_∞ performance, the eigenvalues of graph Laplacian, and the sampling period, for the first-order sampled-data multi-agent network on the directed and the undirected graph, respectively. We derive the optimal sampling period, which is closely related to the minimum and maximum eigenvalues of the graph Laplacian and can ensure that the sampled-data multi-agent network obtains the optimal H_∞ performance. Furthermore, we reveal the relation between the H_∞ performance of the continuous-time multi-agent network and that of the corresponding sampled-data multi-agent network. It is shown that the H_∞ performance of the sampled-data multi-agent network is not better than that of the original continuous-time multi-agent network.

3. We propose a simple sufficient condition for the optimal H_∞ performance problem of the sampled-data multi-agent network. It is convenient when the network topology is unknown or the network size is excessive such that the eigenvalues of graph Laplacian are difficult to compute. Furthermore, a necessary and sufficient condition is developed for the prescribed H_∞ performance problem of the sampled-data multi-agent network.

The rest of this paper is organized as follows. In Section II, some preliminaries in graph theory and H_∞ control theory are given. The relation between the H_∞ performance and the eigenvalues of graph Laplacian for continuous-time multi-agent networks is studied in Section III. In Section IV, we analyze the H_∞ performance of the sampled-data multi-agent network and some extension issues. Numerical tests are shown in Section V. We conclude our work in Section VI.

Notation: Throughout this paper, $\mathbb{N}$ refers to the set of non-negative integers, $\mathbb{R}^n$ is the n-dimensional real column vector space, $\mathbb{R}^{m\times n}$ is the $m \times n$ real matrix space, and $\mathbb{C}^{m\times n}$ is the $m \times n$ complex matrix space. Let $\mathbf{1}$ and $\mathbf{0}$, respectively, be the all-one and all-zero matrices with appropriate dimensions. Specially, $\mathbf{1}_n$ and $\mathbf{0}_n$ denote the $n \times 1$ all ones and all zeros column vectors, respectively. Denote I_n by the n-dimensional identity matrix. For a matrix X, $X^\top$ denotes its transpose, X^H labels its conjugate transpose, and $\sigma_{max}(X)$ represents its maximum singular value. For a Hermitian matrix X, $\lambda_{max}(X)$ denotes its maximum eigenvalue. $X \in \mathbb{C}^{n\times n}$

is normal if $X^H X = XX^H$. $X \in \mathbb{C}^{n\times n}$ is unitary if $X^H X = XX^H = I_n$. $\mathrm{diag}\{a_1, a_2, \dots, a_n\}$ defines a diagonal matrix whose diagonal elements are $a_1, a_2, \dots, a_n$. Define a set $\mathcal{I}_n = \{1, 2, \dots, n\}$. Null set is denoted by $\emptyset$. For the given sets $\mathcal{S}_1$ and $\mathcal{S}_2$, $\mathcal{S}_1 \cup \mathcal{S}_2$ and $\mathcal{S}_1 \cap \mathcal{S}_2$ represent the set union and set intersection, respectively. $|\lambda|$ refers to the absolute value of the real number or the modulus of the complex number λ. A complex number $\lambda \in \mathbb{C}$ is denoted by $\lambda = Re(\lambda) + \mathbf{j}Im(\lambda)$, where $Re(\lambda)$ is the real part of λ, $Im(\lambda)$ is the imaginary part of λ, and $\mathbf{j}$ is the imaginary unit. $\mathcal{L}_2[0, \infty)$ denotes the space of square-integrable signals over $[0, \infty)$ and $\ell_2[0, \infty)$ represents the space of square-summable infinite sequences.

II. Preliminaries

A. Graph Theory

Let $\mathcal{G} = (\mathcal{V}, \mathcal{E}, \mathcal{A})$ be a weighted directed graph with n vertices, where $\mathcal{V} = \{v_1, v_2, \dots, v_n\}$ is the set of nodes, $\mathcal{E} \subseteq \mathcal{V} \times \mathcal{V}$ is the set of edges, and $\mathcal{A} = [a_{ij}]_{n\times n}$ is the weighted adjacency matrix with $a_{ij} \geq 0$. An edge of $\mathcal{G}$ is denoted by $\varepsilon_{ij} = (v_i, v_j)$, where v_j is called the parent vertex of v_i and v_i is the child vertex of v_j. $\varepsilon_{ij} \in \mathcal{E} \Leftrightarrow a_{ij} > 0 \Leftrightarrow$ agent i can receive information from agent j. Moreover, assume that $\mathcal{G}$ has no self-cycles for every node, i.e., $a_{ii} = 0$. A *directed path* between two distinct vertices v_i and v_j is a finite-ordered sequence of distinct edges in $\mathcal{G}$ with the form $(v_i, v_{k_1}), (v_{k_1}, v_{k_2}), \dots, (v_{k_l}, v_j)$. $\mathcal{G}$ has a (directed) *spanning tree* if there exists at least one node having a directed path to all the other nodes. The degree matrix $\mathcal{D} = [d_{ij}]_{n\times n}$ is a diagonal matrix with $d_{ii} = \sum_{j=1}^n a_{ij}$. For convenience, let $d_{\max} = \max_{i\in\mathcal{I}_n}\{d_{ii}\}$. $\mathcal{G}$ is called *balanced* if $\sum_{i\neq j} a_{ij} = \sum_{i\neq j} a_{ji}$ for all $i \in \mathcal{I}_n$. The Laplacian matrix associated with graph $\mathcal{G}$ is defined as $L = [l_{ij}]_{n\times n} = \mathcal{D} - \mathcal{A}$, and $L\mathbf{1}_n = \mathbf{0}_n$.

The graph $\mathcal{G}$ is said to be undirected if $\varepsilon_{ij} \in \mathcal{E} \Leftrightarrow \varepsilon_{ji} \in \mathcal{E}$ for $i, j \in \mathcal{I}_n$. If the graph is undirected, the associated adjacency matrix $\mathcal{A}$ is symmetric, i.e., $\mathcal{A} = \mathcal{A}^\top$. An undirected graph is said to be *connected* if there exists a path between any two distinct vertices of the graph.

Lemma 1 ([1], [4]): The directed (undirected) graph $\mathcal{G}$ has a spanning tree (is connected) if and only if the Laplacian matrix L associated with $\mathcal{G}$ has a simple zero eigenvalue with eigenvector $\mathbf{1}_n$. In addition, all the other non-zero eigenvalues have positive real parts (are positive).

Let λ_i, $i \in \mathcal{I}_n$ be the eigenvalues of Laplacian matrix L associated with graph $\mathcal{G}$. For convenience, in terms of Lemma 1, if $\mathcal{G}$ is directed and has a spanning tree, λ_i assume the form $0 = \lambda_1 < Re(\lambda_2) \leq \dots \leq Re(\lambda_n)$. If $\mathcal{G}$ is undirected and connected, suppose that $0 = \lambda_1 < \lambda_2 \leq \dots \leq \lambda_n$.

Lemma 2 ([11], [14]): Let $\Phi_n \in \mathbb{R}^{n\times n}$ be a symmetric matrix in the form of

$$\Phi_n = \begin{bmatrix} \frac{n-1}{n} & -\frac{1}{n} & \cdots & -\frac{1}{n} \\ -\frac{1}{n} & \frac{n-1}{n} & \cdots & -\frac{1}{n} \\ \vdots & \vdots & \ddots & \vdots \\ -\frac{1}{n} & -\frac{1}{n} & \cdots & \frac{n-1}{n} \end{bmatrix}. \tag{1}$$

Then, there exists an orthogonal matrix $Q \in \mathbb{R}^{n\times n}$ such that

$$Q^\top \Phi_n Q = \bar{\Phi}_n = \begin{bmatrix} I_{n-1} & \mathbf{0}_{n-1} \\ \mathbf{0}_{n-1}^\top & 0 \end{bmatrix},$$

where $Q = \begin{bmatrix} Q_1 & Q_2 \end{bmatrix}$ and $Q_2 = \frac{\mathbf{1}_n}{\sqrt{n}}$ is the last column of Q. Let $\mathcal{G}$ be a directed graph with a normal Laplacian matrix $X \in \mathbb{R}^{n\times n}$, which has a spanning tree. Then, we have

$$Q^\top X Q = \bar{X} = \begin{bmatrix} \bar{X}_1 & \mathbf{0}_{n-1} \\ \mathbf{0}_{n-1}^\top & 0 \end{bmatrix},$$

where $\bar{X}_1 \in \mathbb{R}^{(n-1)\times(n-1)}$ is also a normal matrix and has the same eigenvalues as X but the zero eigenvalue.

B. H_∞ Performance Index

In this subsection, we introduce some basic conceptions in H_∞ control theory. More details are available in [30]–[32].

Consider the following continuous-time system

$$\begin{cases} \dot{x}(t) = A_1 x(t) + B_1 u(t) + E_1 \omega(t), \\ y(t) = C_1 x(t), \\ x(0) = 0, \end{cases} \tag{2}$$

where $x(t) \in \mathbb{R}^n$ is the state, $u(t) \in \mathbb{R}^p$ is the control input taking the form of $u(t) = K_1 x(t)$, $y(t) \in \mathbb{R}^q$ is the output, $\omega(t) \in \mathbb{R}^m$ is the external disturbance satisfying $\omega(t) \in \mathcal{L}_2[0, \infty)$, and A_1, B_1, E_1, C_1 are constant matrices with appropriate dimensions. Let the controller $u(t) = K_1 x(t)$ stabilize system (2). Then we can get the transfer matrix

$$T_1(s) = C_1(sI_n - A_1 - B_1K_1)^{-1}E_1$$

from disturbance $\omega(t)$ to output $y(t)$.

If the quantity we are interested in is the $\mathcal{L}_2$ gain

$$\gamma_1 = \sup_{\substack{\omega(t)\neq 0 \\ \omega(t)\in\mathcal{L}_2[0,\infty)}} \sqrt{\frac{\int_0^\infty y^\top(t)y(t)\,\mathrm{d}t}{\int_0^\infty \omega^\top(t)\omega(t)\,\mathrm{d}t}},$$

we get a disturbance-to-output (D2O) performance index γ_1. The following property is useful.

Property 1 ([31]): If $u(t) = K_1 x(t)$ stabilizes system (2), then

$$\gamma_1 = \|T_1(s)\|_\infty,$$

where $\|T_1(s)\|_\infty = \sup_{v\in\mathbb{R}} \sigma_{max}\left[T_1(\mathbf{j}v)\right]$ is the H_∞ norm of $T_1(s)$.

Clearly, smaller $\|T_1(s)\|_\infty$ means better ability of system output to suppress the disturbance.

Definition 1: When $u(t) = K_1 x(t)$ stabilizes system (2), $\|T_1(s)\|_\infty$ is termed the D2O H_∞ performance index.

Moreover, if the quantity we are interested in is

$$\gamma_2 = \sup_{\substack{\omega(t)\neq 0 \\ \omega(t)\in\mathcal{L}_2[0,\infty)}} \sqrt{\frac{\int_0^\infty y^\top(t)y(t) + u^\top(t)u(t)\,\mathrm{d}t}{\int_0^\infty \omega^\top(t)\omega(t)\,\mathrm{d}t}},$$

we get another performance index γ_2.

Let $z(t) = [y^\top(t), u^\top(t)]^\top$, which is termed combined output. Then, we can obtain the transfer matrix

$$T_2(s) = [C_1^\top, K_1^\top]^\top(sI_n - A_1 - B_1K_1)^{-1}E_1$$

from disturbance $\omega(t)$ to combined output $z(t)$. There holds the following property.

Property 2: If $u(t) = K_1x(t)$ stabilizes system (2), then

$$\gamma_2 = \|T_2(s)\|_\infty,$$

where $\|T_2(s)\|_\infty = \sup_{v\in\mathbb{R}} \sigma_{max}\left[T_2(\mathbf{j}v)\right]$ is the H_∞ norm of $T_2(s)$.

Definition 2: When $u(t) = K_1x(t)$ stabilizes system (2), $\|T_2(s)\|_\infty$ is termed the disturbance-to-combined-output (D2CO) H_∞ performance index.

Clearly, $\|T_2(s)\|_\infty$ represents the anti-disturbance ability of combined output. And both $\|T_1(s)\|_\infty$ and $\|T_2(s)\|_\infty$ can be used to characterize the H_∞ performance of system (2).

Consider the following discrete-time system

$$\begin{cases} x(k+1) = A_2x(k) + B_2u(k) + E_2\omega(k), \\ y(k) = C_2x(k), \\ x(0) = 0, \end{cases} \tag{3}$$

where $x(k) \in \mathbb{R}^n$ is the state, $u(k) \in \mathbb{R}^p$ is the control input taking the form of $u(k) = K_2x(k)$, $y(k) \in \mathbb{R}^q$ is the output, $\omega(k) \in \mathbb{R}^m$ is the external disturbance satisfying $\omega(k) \in \ell_2[0,\infty)$, and A_2, B_2, E_2, C_2 are constant matrices with appropriate dimensions. Let the controller $u(k) = K_2x(k)$ stabilize system (3). Then we can get the transfer matrix

$$T_1(z) = C_2(zI_n - A_2 - B_2K_2)^{-1}E_2$$

from disturbance $\omega(k)$ to output $y(k)$.

If the quantity we are interested in is the ℓ_2 gain

$$\rho_1 = \sup_{\substack{\omega(k)\neq 0\\ \omega(k)\in\ell_2[0,\infty)}} \sqrt{\frac{\sum_{k=0}^{\infty} y^\top(k)y(k)}{\sum_{k=0}^{\infty}\omega^\top(k)\omega(k)}},$$

we get a D2O performance index ρ_1. The following property is useful.

Property 3 ([32]): If $u(k) = K_2x(k)$ stabilizes system (3), then

$$\rho_1 = \|T_1(z)\|_\infty,$$

where $\|T_1(z)\|_\infty = \sup_{v\in[0,2\pi]} \sigma_{max}\left[T_1(\mathrm{e}^{\mathbf{j}v})\right]$ is the H_∞ norm of $T_1(z)$.

Clearly, smaller $\|T_1(z)\|_\infty$ means better ability of system output to suppress the disturbance.

Definition 3: When $u(k) = K_2x(k)$ stabilizes system (3), $\|T_1(z)\|_\infty$ is termed the D2O H_∞ performance index.

Moreover, if the quantity we are interested in is

$$\rho_2 = \sup_{\substack{\omega(k)\neq 0\\ \omega(k)\in\ell_2[0,\infty)}} \sqrt{\frac{\sum_{k=0}^{\infty}\left[y^\top(k)y(k) + u^\top(k)u(k)\right]}{\sum_{k=0}^{\infty}\omega^\top(k)\omega(k)}},$$

we get another performance index ρ_2.

Let $z(k) = [y^\top(k), u^\top(k)]^\top$, which is termed combined output. Then, we can obtain the transfer matrix

$$T_2(z) = [C_2^\top, K_2^\top]^\top(sI_n - A_2 - B_2K_2)^{-1}E_2$$

from disturbance $\omega(k)$ to combined output $z(k)$. There holds the following property.

Property 4: If $u(t) = K_1x(t)$ stabilizes system (3), then

$$\rho_2 = \|T_2(z)\|_\infty,$$

where $\|T_2(z)\|_\infty = \sup_{v\in[0,2\pi]} \sigma_{max}\left[T_2(\mathrm{e}^{\mathbf{j}v})\right]$ is the H_∞ norm of $T_2(z)$.

Definition 4: When $u(k) = K_2x(k)$ stabilizes system (3), $\|T_2(z)\|_\infty$ is termed the D2CO H_∞ performance index.

Clearly, $\|T_2(z)\|_\infty$ represents the anti-disturbance ability of combined output. And both $\|T_1(z)\|_\infty$ and $\|T_2(z)\|_\infty$ can be used to character the H_∞ performance of system (3).

III. Analysis of H_∞ Performance for Continuous-Time Multi-Agent Networks

In this section, we build the relation between the H_∞ performance and the eigenvalues of graph Laplacian for continuous-time multi-agent networks.

Consider a multi-agent network consisting of n agents. The dynamics of each agent is given as follows

$$\dot{x}_i(t) = u_i(t) + \omega_i(t),\ i \in \mathcal{I}_n, \tag{4}$$

where $x_i(t) \in \mathbb{R}$ is the state, $u_i(t) \in \mathbb{R}$ is the control input and $\omega_i(t) \in \mathbb{R}$ is the external disturbance of the i_{th} agent. In addition, assume that $\omega_i(t) \in \mathcal{L}_2[0,\infty)$, i.e., $\int_0^\infty \omega_i^2(t)\,\mathrm{d}t < \infty$. These agents interact in a network described by a weighted graph $\mathcal{G}$ and abide by the following continuous-time consensus protocol

$$u_i(t) = \sum_{j=1}^{n} a_{ij}[x_j(t) - x_i(t)],\ i \in \mathcal{I}_n, \tag{5}$$

where a_{ij} is the $(i,j)_{\text{th}}$ entry of the weighted adjacency matrix $\mathcal{A}$ associated with graph $\mathcal{G}$. Substituting (5) into (4) gives the compact form

$$\dot{X}(t) = U(t) + \Omega(t) = -LX(t) + \Omega(t), \tag{6}$$

where $X(t) = [x_1(t), \ldots, x_n(t)]^\top$, $U(t) = [u_1(t), \ldots, u_n(t)]^\top$, $\Omega(t) = [\omega_1(t), \ldots, \omega_n(t)]^\top$ and L is the Laplacian matrix whose $(i,j)_{\text{th}}$ entry is given by

$$l_{ij} = \begin{cases} \sum_{j=1}^{n} a_{ij} & i = j, \\ -a_{ij} & i \neq j. \end{cases}$$

It is well known that system (6) can reach consensus under $\omega_i(t) = 0$, $\forall i \in \mathcal{I}_n$, i.e.,

$$\lim_{t\to\infty}[x_i(t) - x_j(t)] = 0,\ \forall i, j \in \mathcal{I}_n \tag{7}$$

for any initial condition $X(0)$ if and only if the directed (undirected) graph $\mathcal{G}$ has a spanning tree (is connected) [33]. However, when $\omega_i(t) \neq 0$, $\exists i \in \mathcal{I}_n$, external disturbances may make agents deviate from consensus or damage some expected performance. To measure the disagreement degree, we define the consensus error as follows:

$$e_i(t) = x_i(t) - \frac{1}{n}\sum_{j=1}^{n} x_j(t),\ i \in \mathcal{I}_n. \tag{8}$$

Then, we get the compact form of consensus error

$$e(t) = X(t) - \frac{\mathbf{1}_n}{n}\sum_{j=1}^{n} x_j(t) = \Phi_n X(t), \tag{9}$$

where $e(t) = [e_1(t), \dots, e_n(t)]^\top$ and Φ_n is defined in (1). It is evident that (7) holds if and only if $\lim_{t\to\infty} e(t) = \mathbf{0}_n$. Then the vector $e(t)$ can be used to characterize the disagreement behavior of all agents under external disturbances. For system (6), the quantity we are interested in is the following performance index

$$\gamma = \sup_{\substack{\Omega(t)\neq 0 \\ \Omega(t)\in\mathcal{L}_2[0,\infty)}} \sqrt{\frac{\int_0^\infty e^\top(t)e(t) + U^\top(t)U(t)\,\mathrm{d}t}{\int_0^\infty \Omega^\top(t)\Omega(t)\,\mathrm{d}t}} \tag{10}$$

which represents the influence of disturbances on consensus and control effort together. For convenience, let $J_c = \int_0^\infty e^\top(t)e(t) + U^\top(t)U(t)\,\mathrm{d}t$ and $W_c = \int_0^\infty \Omega^\top(t)\Omega(t)\,\mathrm{d}t$. However, we cannot directly compute γ in time-domain since it is impossible to enumerate innumerable disturbances in $\mathcal{L}_2[0,\infty)$. Accordingly, we make the following treatment.

Define a combined output

$$Y(t) = \begin{bmatrix} e(t) \\ U(t) \end{bmatrix} = \begin{bmatrix} \Phi_n \\ -L \end{bmatrix} X(t) \tag{11}$$

that is nominal for system (6). Then, the transfer matrix from disturbance $\Omega(t)$ to combined output $Y(t)$ is

$$T_{Y\Omega}(s) = \begin{bmatrix} \Phi_n \\ -L \end{bmatrix} (sI_n + L)^{-1}. \tag{12}$$

According to Property 2 and Definition 2, we can obtain

$$\gamma = \|T_{Y\Omega}(s)\|_\infty \tag{13}$$

where $\|T_{Y\Omega}(s)\|_\infty = \sup_{v\in\mathbb{R}} \sigma_{max}\left[T_{Y\Omega}(\mathbf{j}v)\right]$ is the D2CO H_∞ performance index of system (6)-(11). Therefore, investigating γ can be transformed to analyze the D2CO H_∞ performance $\|T_{Y\Omega}(s)\|_\infty$ which is more tractable by using frequency-domain analysis.

Remark 1: Note the fact that $\|T_{Y\Omega}(s)\|_\infty$ is not well-defined for all network topologies. However, $\|T_{Y\Omega}(s)\|_\infty$ is always well-defined for consensus networks because the marginally stable mode of system (6)-(11) is unobservable from output $Y(t)$ as long as the directed (undirected) graph $\mathcal{G}$ has a spanning tree (is connected) [34].

Since $T_{Y\Omega}(s)$ depends on L, our goal is to explore the relation between H_∞ performance $\|T_{Y\Omega}(s)\|_\infty$ and the eigenvalues of L to provide guidelines for designing network topology with optimal H_∞ performance. The following result is stated for a class of directed graphs.

Theorem 1: Let $\mathcal{G}$ be a directed graph with a normal Laplacian matrix L. If $\mathcal{G}$ has a spanning tree, then the D2CO H_∞ performance of system (6)-(11) is

$$\|T_{Y\Omega}(s)\|_\infty = \max_{i=2,\dots,n} \sqrt{\frac{1+|\lambda_i|^2}{Re^2(\lambda_i)}} > 1.$$

Proof: The proof is presented in Appendix A. ■

The above result can be reduced to the undirected graph case which is described in the following.

Corollary 1: Let $\mathcal{G}$ be a connected undirected graph with a Laplacian matrix L. Then, the D2CO H_∞ performance of system (6)-(11) is

$$\|T_{Y\Omega}(s)\|_\infty = \sqrt{1 + \frac{1}{\lambda_2^2}} > 1. \tag{14}$$

Proof: Since $\mathcal{G}$ is undirected, L is symmetric and hence normal. In addition, $\mathcal{G}$ must has a spanning tree because $\mathcal{G}$ is connected. In terms of Theorem 1, the relation between H_∞ performance and eigenvalues of L for system (6)-(11) is $\|T_{Y\Omega}(s)\|_\infty = \max_{i=2,\dots,n} \sqrt{1+\frac{1}{\lambda_i^2}} > 1$. It follows from $\lambda_2 \le \dots \le \lambda_n$ that $\|T_{Y\Omega}(s)\|_\infty = \sqrt{1+\frac{1}{\lambda_2^2}} > 1$. The proof is completed. ■

Specially, if we take no account of the control effort, output (11) becomes

$$Y(t) = e(t) = \Phi_n X(t). \tag{15}$$

Then, the D2CO H_∞ performance in Theorem 1 becomes the D2O H_∞ performance

$$\|T_{Y\Omega}(s)\|_\infty = \frac{1}{Re(\lambda_2)}. \tag{16}$$

The D2CO H_∞ performance in Corollary 1 is reduced to the D2O H_∞ performance

$$\|T_{Y\Omega}(s)\|_\infty = \frac{1}{\lambda_2} \tag{17}$$

obtained in [20], [21]. Therefore, our results are more general. Furthermore, compared with [22], the expressions of H_∞ performance derived in this paper are more explicit such that it is conducive to design the optimal consensus network against disturbances.

Remark 2: Corollary 1 shows a counter-intuitive fact that undirected networks with different topological structures but the same λ_2 have the same disturbance rejection capability. They indeed generate different levels of amplification for a given disturbance. However, the H_∞ performance represents the worst level of amplification for all disturbances in $\mathcal{L}_2[0,\infty)$, and Corollary 1 shows that it only depends on λ_2. Therefore, in the sense of H_∞ performance, undirected networks with different structures but the same λ_2 have the same disturbance rejection capability. If we use other performance indices, the results may be different.

Remark 3: The expressions (14) and (17) are useful to design the optimal consensus network topology against external disturbances. In the set of connected undirected networks with 0-1 edge weights composed of n agents, the complete graph is the optimal network topology since it has the largest λ_2. For any connected undirected network, we can magnify the weights of each edge by an equal scaling factor $\alpha > 1$ such that the Laplacian matrix L becomes αL. Then increasing α makes λ_2 increase, hence improving the H_∞ performance. As long as α is large enough, any undirected network is able to close to optimal H_∞ performance. In addition, as λ_2 increases in (14), the influence of disturbances on consensus gradually diminishes to almost disappear, but the influence on control cost always exists and is invariable. Therefore, if λ_2 is large enough, (14) is close to H_∞ performance limits 1 and almost completely reflects the influence of disturbances on control effort.

IV. Analysis of H_∞ Performance for Sampled-Data Multi-Agent Networks

In this section, we will explore the H_∞ performance of sampled-data multi-agent consensus network. We intend to derive the optimal sampling period and reveal the relation between the H_∞ performance of continuous-time multi-agent consensus network and that of corresponding sampled-data multi-agent consensus network. Before presenting our results, we need to introduce the sampled-data multi-agent network model. The continuous-time linear consensus protocol (5) is periodically sampled by using a zero-order hold circuit with a sampling period $h > 0$. Then, discretizing (4) yields the following sampled-data multi-agent system:

$$\begin{cases} x_i(t_{k+1}) = x_i(t_k) + hu_i(t_k) + h\omega_i(t_k), \\ u_i(t) = \sum_{j=1}^{n} a_{ij}[x_j(t_k) - x_i(t_k)], \text{ if } t \in [t_k, t_{k+1}), \\ t_k = kh, \ k \in \mathbb{N}, \ i \in \mathcal{I}_n, \end{cases} \tag{18}$$

where $x_i(t_k) \in \mathbb{R}$, $u_i(t_k) \in \mathbb{R}$ and $\omega_i(t_k) \in \mathbb{R}$ denote, respectively, the state, control input and sampled disturbance signal of the i_{th} agent. Obviously, $\omega_i(t) \in \mathcal{L}_2[0,\infty)$ renders $\omega_i(t_k) \in \ell_2[0,\infty)$, i.e., $\sum_{k=0}^{\infty} \omega_i^2(t_k) < \infty$. Then rewriting (18) gives the collective dynamics

$$X(t_{k+1}) = (I_n - hL)X(t_k) + h\Omega(t_k), \tag{19}$$

where $X(t_k) = [x_1(t_k), \ldots, x_n(t_k)]^\top$, $U(t_k) = [u_1(t_k), \ldots, u_n(t_k)]^\top$, $\Omega(t_k) = [\omega_1(t_k), \ldots, \omega_n(t_k)]^\top$ and L is the Laplacian matrix defined in (6). There is no doubt that system (19) reaches consensus under $\omega_i(t_k) = 0$, $\forall k \in \mathbb{N}$, $\forall i \in \mathcal{I}_n$ for any initial condition $X(t_0)$ if and only if the directed (undirected) graph $\mathcal{G}$ has a directed spanning tree (is connected) and the sampling period h satisfies

$$0 < h < \min_{i=2,\ldots,n} \frac{2Re(\lambda_i)}{|\lambda_i|^2} \ (0 < h < \frac{2}{\lambda_n})$$

[26]. When disturbances occur, we define the consensus error

$$e_i(t_k) = x_i(t_k) - \frac{1}{n}\sum_{j=1}^{n} x_j(t_k), \ i \in \mathcal{I}_n \tag{20}$$

to measure the disagreement degree of each agent. Then aggregate errors into a vector

$$e(t_k) = X(t_k) - \frac{\mathbf{1}_n}{n}\sum_{j=1}^{n} x_j(t_k) = \Phi_n X(t_k), \tag{21}$$

where $e(t_k) = [e_1(t_k), \ldots, e_n(t_k)]^\top$.

In this paper, we are interested to find the optimal sampling period for multi-agent networks, and investigate whether sampling control deteriorate or improve the H_∞ performance. Since we use zero-order hold circuit to realize periodic sampling, $J_c = \int_0^\infty e^\top(t)e(t) + U^\top(t)U(t)\,\mathrm{d}t$ and $W_c = \int_0^\infty \Omega^\top(t)\Omega(t)\,\mathrm{d}t$ for system (6) can be respectively approximated as

$$\begin{aligned} J_d(h) &= \sum_{k=0}^{\infty}(t_{k+1} - t_k)\left[e^\top(t_k)e(t_k) + U^\top(t_k)U(t_k)\right] \\ &= h\sum_{k=0}^{\infty}\left[e^\top(t_k)e(t_k) + U^\top(t_k)U(t_k)\right] \end{aligned}$$

and

$$W_d(h) = \sum_{k=0}^{\infty}(t_{k+1}-t_k)\left[\Omega^\top(t_k)\Omega(t_k)\right] = h\sum_{k=0}^{\infty}\Omega^\top(t_k)\Omega(t_k).$$

It follows from $\lim_{h\to 0} J_d(h) = J_c$ and $\lim_{h\to 0} W_d(h) = W_c$ that J_c and $J_d(h)$, W_c and $W_d(h)$ are both comparable. Therefore, it is reasonable to reveal the effect of sampling control on H_∞ performance by comparing performance index γ and its counterpart

$$\rho_h = \sup_{\substack{\Omega(t_k)\neq 0 \\ \Omega(t_k)\in\ell_2[0,\infty)}} \sqrt{\frac{h\sum_{k=0}^{\infty}\left[e^\top(t_k)e(t_k) + U^\top(t_k)U(t_k)\right]}{h\sum_{k=0}^{\infty}\Omega^\top(t_k)\Omega(t_k)}} \tag{22}$$

for sampled-data multi-agent system (19). However, it is hard to perform in time-domain. Furthermore, performance index ρ_h is indeed related to the sampling period but the optimal sampling period is also difficult to determined in time-domain. Accordingly, we make the following treatment.

Construct the following combined output

$$Y(t_k) = \begin{bmatrix} e(t_k) \\ U(t_k) \end{bmatrix} = \begin{bmatrix} \Phi_n \\ -L \end{bmatrix} X(t_k) \tag{23}$$

that is nominal for system (19). Then, the transfer matrix from sampled disturbance $\Omega(t_k)$ to combined output $Y(t_k)$ is

$$T_{Y\Omega}(z) = h\begin{bmatrix} \Phi_n \\ -L \end{bmatrix}(zI_n - I_n + hL)^{-1}.$$

Noticing that in (22), constants h in the numerator and the denominator can be simultaneously eliminated, we have

$$\rho_h = \sup_{\substack{\Omega(t_k)\neq 0 \\ \Omega(t_k)\in\ell_2[0,\infty)}} \sqrt{\frac{\sum_{k=0}^{\infty}\left[e^\top(t_k)e(t_k) + U^\top(t_k)U(t_k)\right]}{\sum_{k=0}^{\infty}\Omega^\top(t_k)\Omega(t_k)}}.$$

Then, according to Property 4 and Definition 4, we can obtain

$$\rho_h = \|T_{Y\Omega}(z)\|_\infty, \tag{24}$$

where $\|T_{Y\Omega}(z)\|_\infty = \sup_{v\in[0,2\pi]}\sigma_{max}\left[T_{Y\Omega}(\mathrm{e}^{\mathrm{j}v})\right]$ is the D2CO H_∞ performance index of system (19)-(23). Therefore, we can study the optimal sampling period by using frequency-domain analysis. Furthermore, it follows from (13) and (24) that we just need to compare $\|T_{Y\Omega}(s)\|_\infty$ and $\|T_{Y\Omega}(z)\|_\infty$ to reveal the effect of sampling control on H_∞ performance instead of γ and ρ_h, which is more tractable by using frequency-domain analysis. Before the quantitative comparison, we need to determine the analytic expression of $\|T_{Y\Omega}(z)\|_\infty$ as we did for $\|T_{Y\Omega}(s)\|_\infty$. Note that $T_{Y\Omega}(z)$ is related to L and h. We will first study how network topology and sampling period affect the H_∞ performance.

Remark 4: There are no weighting matrices for consensus errors and controls in quadratic performance indices J_c and

$J_d(h)$. Because when we construct combined outputs (11) and (23), adding weighting matrices even if simple diagonal weighting matrices brings asymmetry for matrices Φ_n and L in output matrices such that the spectrum of Laplacian cannot be isolated by orthogonal transformation. Therefore, for matrix-weighted forms of performance indices J_c and $J_d(h)$, the general analytic expressions of H_∞ performance is difficult to build in terms of our current approach.

Remark 5: Besides disturbances, initial conditions also affect combined outputs $Y(t) = [e^\top(t)\ U^\top(t)]^\top$ and $Y(t_k) = [e^\top(t_k)\ U^\top(t_k)]^\top$ and then affect performance indices (10) and (22). However, like most related works [14]–[17], [20]–[24], we only concern the independent influence of external disturbances. Therefore, zero initial conditions are guaranteed to eliminate the influence of initial conditions on performance indices (10) and (22). On the other hand, different with existing works, we aim to obtain the analytic expressions of H_∞ performance indices γ and ρ_h via frequency-domain analysis for $\|T_{Y\Omega}(s)\|_\infty$ and $\|T_{Y\Omega}(z)\|_\infty$. According to H_∞ control theory, (13) and (24) only hold for zero initial conditions. Although some numerical computation methods such as solving Riccati equations [30] or LMIs [18], [19], [35], may be useful to analyze the H_∞ performance under non-zero initial conditions, they are difficult to reveal the quantitative relation between the H_∞ performance, the topological structure of the network, and the sampling period.

A. H_∞ *Performance on Directed and Undirected Graphs*

In this subsection, we derive the quantitative relation between $\|T_{Y\Omega}(z)\|_\infty$, the eigenvalues of L, and the sampling period h, for sampled-data multi-agent system (19)-(23) on directed graphs with normal Laplacian matrix. Then, the result is reduced to the undirected graph case.

Theorem 2: Let $\mathcal{G}$ be a directed graph with a normal Laplacian matrix L. If $\mathcal{G}$ has a spanning tree, Then, the D2CO H_∞ performance of system (19)-(23) is

$$\|T_{Y\Omega}(z)\|_\infty = \max_{i=2,\dots,n} h\sqrt{\frac{1+|\lambda_i|^2}{(1-|\mu_i|)^2}} > 1,$$

where $0 < h < \min\limits_{i=2,\dots,n} \frac{2Re(\lambda_i)}{|\lambda_i|^2}$ and $\mu_i = 1 - h\lambda_i$.

Proof: The proof is provided in Appendix B. ■

Moreover, the result in Theorem 2 is simplified to the undirected graph case which will be used in the next subsection.

Corollary 2: Let $\mathcal{G}$ be a connected undirected graph with a Laplacian matrix L. Then, the D2CO H_∞ performance of system (19)-(23) is

$$\|T_{Y\Omega}(z)\|_\infty = \max\left\{\sqrt{1+\frac{1}{\lambda_2^2}}, h\sqrt{\frac{1+\lambda_n^2}{(2-h\lambda_n)^2}}\right\} > 1, \tag{25}$$

where $0 < h < \frac{2}{\lambda_n}$.

Proof: Since $\mathcal{G}$ is undirected and connected, L is symmetric and hence normal. In addition, the eigenvalues of L are all real such that $0 < h < \frac{2}{\lambda_n} = \min\limits_{i=2,\dots,n} \frac{2Re(\lambda_i)}{|\lambda_i|^2}$. It follows from Theorem 2 that

$$\|T_{Y\Omega}(z)\|_\infty = \max_{i=2,\dots,n} h\sqrt{\frac{1+\lambda_i^2}{(1-|1-h\lambda_i|)^2}} > 1. \tag{26}$$

Note that $0 < h < \frac{2}{\lambda_n}$ leads to $|1-h\lambda_i| < 1, \forall i \in \{2,\dots,n\}$. Let $\mathcal{S}_1$ and $\mathcal{S}_2$ be two sets of λ_i that satisfy $0 \le 1-h\lambda_i < 1$ and $-1 < 1-h\lambda_i < 0$, respectively. Thus, $\mathcal{S} \triangleq \mathcal{S}_1 \cup \mathcal{S}_2 = \{\lambda_2,\dots,\lambda_n\}$ and $\mathcal{S}_1 \cap \mathcal{S}_2 = \emptyset$ hold. For convenience, let

$$g(\lambda_i) = h\sqrt{\frac{1+\lambda_i^2}{(1-|1-h\lambda_i|)^2}}.$$

Then, we will complete the proof by enumeration.

Case (a): $\mathcal{S}_1 = \{\lambda_2,\dots,\lambda_n\}$ and $\mathcal{S}_2 = \emptyset$;

It means that $0 \le 1-h\lambda_i < 1, \forall i \in \{2,\dots,n\}$. Then we have

$$g(\lambda_i) = \sqrt{1+\frac{1}{\lambda_i^2}} > h\sqrt{\frac{1+\lambda_i^2}{(2-h\lambda_i)^2}}.$$

Since $g(\lambda_i)$ decreases as λ_i increases, we conclude that

$$\sqrt{1+\frac{1}{\lambda_2^2}} > \sqrt{1+\frac{1}{\lambda_n^2}} > h\sqrt{\frac{1+\lambda_n^2}{(2-h\lambda_n)^2}}.$$

It follows that $\max_{\lambda_i\in\mathcal{S}} g(\lambda_i) = \max_{\lambda_i\in\mathcal{S}_1} g(\lambda_i) = g(\lambda_2) = \sqrt{1+\frac{1}{\lambda_2^2}}$.

Case (b): $\mathcal{S}_1 = \emptyset$ and $\mathcal{S}_2 = \{\lambda_2,\dots,\lambda_n\}$;

In this case, we get $-1 < 1-h\lambda_i < 0, \forall i \in \{2,\dots,n\}$. Therefore, we can obtain

$$g(\lambda_i) = h\sqrt{\frac{1+\lambda_i^2}{(2-h\lambda_i)^2}} > \sqrt{1+\frac{1}{\lambda_i^2}}.$$

Since $g(\lambda_i)$ is increasing as λ_i is increasing, one can deduce that

$$h\sqrt{\frac{1+\lambda_n^2}{(2-h\lambda_n)^2}} > h\sqrt{\frac{1+\lambda_2^2}{(2-h\lambda_2)^2}} > \sqrt{1+\frac{1}{\lambda_2^2}}.$$

Therefore, it follows that $\max_{\lambda_i\in\mathcal{S}} g(\lambda_i) = \max_{\lambda_i\in\mathcal{S}_2} g(\lambda_i) = g(\lambda_n) = h\sqrt{\frac{1+\lambda_n^2}{(2-h\lambda_n)^2}}$.

Case (c): $\mathcal{S}_1 \ne \emptyset$ and $\mathcal{S}_2 \ne \emptyset$.

Since $\lambda_2 \in \mathcal{S}_1$ and $\lambda_n \in \mathcal{S}_2$ must hold, we have

$$\begin{aligned}\max_{\lambda_i\in\mathcal{S}} g(\lambda_i) &= \max\left\{\max_{\lambda_i\in\mathcal{S}_1} g(\lambda_i), \max_{\lambda_i\in\mathcal{S}_2} g(\lambda_i)\right\} \\ &= \max\left\{\sqrt{1+\frac{1}{\lambda_2^2}}, h\sqrt{\frac{1+\lambda_n^2}{(2-h\lambda_n)^2}}\right\}.\end{aligned}$$

To sum up, we can obtain

$$\begin{aligned}\|T_{Y\Omega}(z)\|_\infty &= \max_{\lambda_i\in\mathcal{S}} g(\lambda_i) \\ &= \max\left\{\sqrt{1+\frac{1}{\lambda_2^2}}, h\sqrt{\frac{1+\lambda_n^2}{(2-h\lambda_n)^2}}\right\} > 1.\end{aligned}$$

The proof is completed. ■

Remark 6: In this paper, the directed graph $\mathcal{G}$ is assumed to have a spanning tree and a normal Laplacian matrix L. It is shown in [11] that if L is normal, $\mathcal{G}$ is balanced but not necessarily vice versa. Therefore, Theorems 1 and

This article has been accepted for publication in IEEE Transactions on Automatic Control. This is the author's version which has not been fully edited and content may change prior to final publication. Citation information: DOI 10.1109/TAC.2023.3342060

2 are only adapted for some balanced graphs. The main difficulty in extending the results to the case of general directed graphs is that most Laplacian matrices associated with directed graphs cannot be orthogonally diagonalized. In this case, the H_∞ performance may be implicitly related to the complex eigenvalues and the eigenvectors of L. Therefore, it is hard to build general analytic expressions of H_∞ performance for all directed graphs. Moreover, for a balanced graph, containing a spanning tree implies being strongly connected [36]. Therefore, first-order multi-agent systems (6) and (19) can both achieve average consensus on strongly connected balanced graphs without disturbances [3]. The above facts mean that consensus errors (8) and (20) are reasonable to measure the deviation from the state of each agent to the average value of all agent states. In addition, we only considered first-order multi-agent networks. The complexity of higher-order dynamics models will increase the difficulty of analysis. We start with a preliminary attempt on first-order dynamics models. It will provide the possibility of further investigating the influence of sampling control on higher-order dynamics models.

B. Optimal H_∞ Performance on Undirected Graphs

In this subsection, we get the optimal sampling period to guarantee that the sampled-data multi-agent system (19)-(23) obtains optimal H_∞ performance on a given undirected graph. We also prove that the H_∞ performance of sampled-data multi-agent system (19)-(23) is not better than that of the continuous-time system (6)-(11) on the same undirected network topology. Some extension issues are also investigated.

Definition 5: Let $\mathcal{G}$ be a connected undirected graph. Then, the optimal H_∞ performance and the optimal sampling period of system (19)-(23) is defined as

$$\|T_{Y\Omega}(z)\|_\infty^* = \min_h \|T_{Y\Omega}(z)\|_\infty$$

and

$$h^* = \max\left\{\arg\min_h \|T_{Y\Omega}(z)\|_\infty\right\},$$

respectively.

Remark 7: In engineering applications, we hope that the system maintains good robustness while a large sampling period is expected to reduce the sampling cost. Thus we call h^* the optimal sampling period.

Theorem 3: Let $\mathcal{G}$ be a connected undirected graph. Then, there exists a unique optimal sampling period

$$h^*=\begin{cases}\dfrac{1}{\lambda_2} & \lambda_2=\lambda_n,\\ \dfrac{2\lambda_n+2\lambda_2^2\lambda_n-2\lambda_2\sqrt{1+\lambda_2^2+\lambda_n^2+\lambda_2^2\lambda_n^2}}{\lambda_n^2-\lambda_2^2} & \lambda_2\neq\lambda_n,\end{cases}$$

such system (19)-(23) obtains the optimal H_∞ performance

$$\|T_{Y\Omega}(z)\|_\infty^* = \sqrt{1+\frac{1}{\lambda_2^2}}.$$

Furthermore, the optimal H_∞ performance is maintained when $0<h<h^*$.

Proof: The proof is divided into two main steps.

Step I: Proving the existence and the uniqueness of the optimal sampling period h^*.

By inspecting (25), let

$$p(h)=\sqrt{1+\frac{1}{\lambda_2^2}} \tag{27}$$

and

$$q(h)=h\sqrt{\frac{1+\lambda_n^2}{(2-h\lambda_n)^2}}. \tag{28}$$

Note that $p(h)$ is constant and $q(h)$ is monotonically increasing as h is increasing. Therefore, $p(h)-q(h)$ is monotonically decreasing. In addition, we have $\lim_{h\to 0} p(h)-q(h)>0$, $\lim_{h\to\frac{2}{\lambda_n}} p(h)-q(h)<0$. Thus, $p(h)-q(h)=0$ which is equivalent to

$$(\lambda_n^2-\lambda_2^2)h^2-(4\lambda_n+4\lambda_2^2\lambda_n)h+4+4\lambda_2^2=0 \tag{29}$$

has only one positive real root over $(0,\frac{2}{\lambda_n})$ denoted by h_c. Then, (25) can be expressed as a piecewise continuous function

$$\|T_{Y\Omega}(z)\|_\infty=\varphi(h)=\begin{cases}p(h) & 0<h\le h_c,\\ q(h) & h_c\le h<\dfrac{2}{\lambda_n}.\end{cases} \tag{30}$$

Since $\varphi(h)$ is non-decreasing, the optimal H_∞ performance

$$\|T_{Y\Omega}(z)\|_\infty^*=\min_{h\in(0,\frac{2}{\lambda_n})}\varphi(h)=p(h)=\sqrt{1+\frac{1}{\lambda_2^2}}$$

is obtained when $0<h\le h_c$. According to Definition 5, the optimal sampling period is $h^*=h_c$.

Fig. 1 shows the H_∞ performance of system (19)-(23). The red line and blue line, respectively, refer to trajectories of $p(h)$ and $q(h)$. The solid line depicts the trajectory of H_∞ performance $\|T_{Y\Omega}(z)\|_\infty=\varphi(h)$ with respect to h. As one can see that the optimal sampling period h^* is unique. Moreover, the optimal H_∞ performance can be maintained as long as $0<h<h^*$.

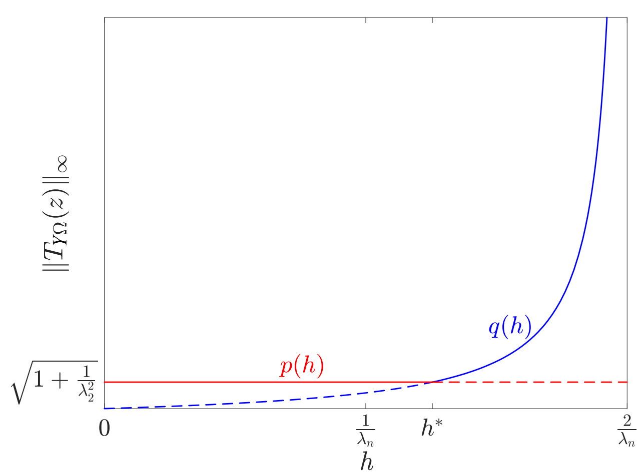

Fig. 1: Trajectory of H_∞ performance.

Step II: Computing h^* under two cases.

Case (i): $\lambda_2=\lambda_n$;

In this case, (29) becomes

$$-(4\lambda_2+4\lambda_2^3)h+4+4\lambda_2^2=0. \tag{31}$$

Solving (31) yields $h^*=\frac{1}{\lambda_2}<\frac{2}{\lambda_n}$.

Case (ii): $\lambda_2\neq\lambda_n$.

The solutions of (29) are

$$h_1=\frac{2\lambda_n+2\lambda_2^2\lambda_n+2\lambda_2\sqrt{1+\lambda_2^2+\lambda_n^2+\lambda_2^2\lambda_n^2}}{\lambda_n^2-\lambda_2^2}>\frac{2}{\lambda_n},$$

$$h_2=\frac{2\lambda_n+2\lambda_2^2\lambda_n-2\lambda_2\sqrt{1+\lambda_2^2+\lambda_n^2+\lambda_2^2\lambda_n^2}}{\lambda_n^2-\lambda_2^2}<\frac{2}{\lambda_n}.$$

Since $0<h<\frac{2}{\lambda_n}$, the optimal sampling period is $h^*=h_2$. ■

Remark 8: Theorem 3 shows a counter-intuitive fact that the H_∞ performance cannot be improved via reducing the sampling time when it is less than some threshold. This may result from two aspects. On the one hand, we use H_∞ performance index to measure the influence of disturbances. If we employ other performance indices, the result may be different. On the other hand, it may be related to the sampling method. In this paper, we only considered the simple periodic sampling with the zero-order hold circuit. If we employ higher-order hold circuits or other sampling methods [29] such as aperiodic sampling, stochastic sampling, and event-triggered sampling, the relation between H_∞ performance and sampling period will be totally different. Therefore, it may require further analysis for the range of sampling periods or the expected value of sampling periods.

It is observed from Theorem 3 that system (19)-(23) at most maintains the same H_∞ performance as system (6)-(11) by adjusting sampling period within $(0,h^*]$ on the same connected undirected graph, i.e., $\|T_{Y\Omega}(z)\|_\infty^*=\|T_{Y\Omega}(s)\|_\infty=\sqrt{1+\frac{1}{\lambda_2^2}}$. Therefore, we have the following significant statement which is also illustrated in Fig. 1.

Corollary 3: The H_∞ performance of the sampled-data multi-agent system (19)-(23) is not better than that of the continuous-time multi-agent system (6)-(11) on the same connected undirected graph.

Remark 9: Theorem 3 answers the question 1) raised in Section I. There exists the optimal sampling period such that the first-order sampled-data multi-agent network obtains the optimal H_∞ performance. Corollary 3 answers the question 2) raised in Section I. It is shown that for the first-order continuous-time multi-agent consensus network, periodic sampling cannot improve and at most maintains the H_∞ performance

Unfortunately, the optimal sampling period h^* is reliant on λ_2 and λ_n which are hard to obtain when the network topology is unknown or the network size is excessive. By contrast, $d_{\max}$ is easier to obtain. Therefore, the following result is deduced.

Corollary 4: Let $\mathcal{G}$ be a connected undirected graph. Then, system (19)-(23) obtains the optimal H_∞ performance

$$\|T_{Y\Omega}(z)\|_\infty^*=\sqrt{1+\frac{1}{\lambda_2^2}}$$

if

$$0<h\leq\frac{1}{2d_{\max}}. \tag{32}$$

Proof: Combining (27) with (28) yields $p(\frac{1}{\lambda_n})-q(\frac{1}{\lambda_n})\geq 0$. Since $p(h)-q(h)$ is monotonically decreasing and $p(h^*)-q(h^*)=0$, we have $\frac{1}{\lambda_n}\leq h^*$ which is also illustrated in Fig. 1. In addition, we can obtain $\lambda_n\leq 2d_{\max}$ by using Geršgorin disk theorem. It follows that $\frac{1}{2d_{\max}}\leq h^*$. According to Theorem 3, system (19)-(23) can achieve the optimal H_∞ performance $\|T_{Y\Omega}(z)\|_\infty^*=\sqrt{1+\frac{1}{\lambda_2^2}}$ if $0<h\leq\frac{1}{2d_{\max}}$. ■

More specifically, for the connected undirected graph with 0-1 edge weights, (32) can be reduced to $0<h\leq\frac{1}{n}$ because λ_n is never larger than n [37].

Naturally, we also state a necessary and sufficient condition such that the sampled-data multi-agent network obtains the prescribed H_∞ performance.

Corollary 5: Let $\mathcal{G}$ be a connected undirected graph. Then, system (19)-(23) obtains the prescribed H_∞ performance $\|T_{Y\Omega}(z)\|_\infty<\gamma$ ($\gamma>\sqrt{1+\frac{1}{\lambda_2^2}}$) if and only if

$$0<h<\frac{2\gamma^2\lambda_n-2\gamma\sqrt{1+\lambda_n^2}}{(\gamma^2-1)\lambda_n^2-1}.$$

Proof: It is inferred from (30) that $\|T_{Y\Omega}(z)\|_\infty<\gamma$ holds if and only if $q(h)<\gamma$, which can be solved as $h>\frac{2\gamma^2\lambda_n+2\gamma\sqrt{1+\lambda_n^2}}{(\gamma^2-1)\lambda_n^2-1}>\frac{2}{\lambda_n}$ and $h<\frac{2\gamma^2\lambda_n-2\gamma\sqrt{1+\lambda_n^2}}{(\gamma^2-1)\lambda_n^2-1}<\frac{2}{\lambda_n}$. Since sampling period should satisfies $0<h<\frac{2}{\lambda_n}$, it can be readily concluded that $\|T_{Y\Omega}(z)\|_\infty<\gamma$ if and only if $0<h<\frac{2\gamma^2\lambda_n-2\gamma\sqrt{1+\lambda_n^2}}{(\gamma^2-1)\lambda_n^2-1}$. ■

Remark 10: Most works derived sufficient conditions in the form of LMI for the prescribed H_∞ performance problem, while we provide another concise scheme which is sufficient and necessary.

So far, we have investigated the D2CO H_∞ performance on both consensus and control effort. If we only consider the influence of disturbances on consensus, output (23) becomes

$$y(t_k)=e(t_k)=\Phi_n X(t_k) \tag{33}$$

and the D2CO H_∞ performance of system (19)-(23) is reduced to the D2O H_∞ performance of system (19)-(33). Then the optimal sampling period and the optimal H_∞ performance of system (19)-(33) are given in the following.

Corollary 6: Let $\mathcal{G}$ be a connected undirected graph. Then, there exists a unique optimal sampling period $h^*=\frac{2}{\lambda_2+\lambda_n}$ such that system (19)-(33) obtains the optimal H_∞ performance $\|T_{Y\Omega}(z)\|_\infty^*=\frac{1}{\lambda_2}$.

Proof: Similar to the proofs of Corollary 2 and Theorem 3, we can prove that the D2O H_∞ performance of system (19)-(33) is

$$\|T_{Y\Omega}(z)\|_\infty=\max\left\{\frac{1}{\lambda_2},\frac{h}{2-h\lambda_n}\right\}, \tag{34}$$

and there exists the optimal sampling period h^* such that system (19)-(33) obtains the optimal H_∞ performance $\|T_{Y\Omega}(z)\|_\infty^*=\min_{h\in(0,\frac{2}{\lambda_n})}\|T_{Y\Omega}(z)\|_\infty=\frac{1}{\lambda_2}$. The optimal sampling period h^* is unique and satisfies $\frac{1}{\lambda_2}=\frac{h^*}{2-h^*\lambda_n}$. Therefore, we have $h^*=\frac{2}{\lambda_2+\lambda_n}$. ■

Combining (17) with Corollary 6, we can find that the sampled-data multi-agent system (19)-(33) at most maintains the same H_∞ performance as the continuous-time system

(6)-(15) on the same connected undirected graph. Moreover, Corollary 4 is still feasible for system (19)-(33). Similar to Corollary 5, we can infer that the sampled-data system (19)-(33) obtains the prescribed H_∞ performance $\|T_{Y\Omega}(z)\|_\infty < \gamma$ ($\gamma > \frac{1}{\lambda_2}$) if and only if $0 < h < \frac{2\gamma}{1+\gamma\lambda_n}$.

Remark 11: The classic discrete-time multi-agent system [3] in the presence of disturbances is $X(k+1) = (I_n - hL)X(k) + \Omega(k)$. Compared with sampled-data multi-agent system (19), the disturbances are directly injected rather than sampling such that there is no step-size h before $\Omega(k)$. For the classic discrete-time multi-agent system, the H_∞ performance on the directed graph which contains a spanning tree and the normal Laplacian matrix becomes $\|T_{Y\Omega}(z)\|_\infty = \max_{i=2,\ldots,n} \sqrt{\frac{1+(h|\lambda_i|)^2}{(1-|\mu_i|)^2}} \geq \sqrt{2}$. The H_∞ performance on the connected undirected graph is $\|T_{Y\Omega}(z)\|_\infty = \max\left\{\sqrt{1+\frac{1}{(h\lambda_2)^2}}, \sqrt{\frac{1+(h\lambda_n)^2}{(2-h\lambda_n)^2}}\right\} \geq \sqrt{2}$. Furthermore, by the similar approach of proving Theorem 3, we can prove that the optimal step-size h^* still exists.

V. Numerical Tests

We show our results on some well-known graphs. Consider some graphs with normal Laplacian matrices and 0-1 edge weights, which include undirected complete graphs $\mathcal{G}_{uc}$, undirected path graphs $\mathcal{G}_{up}$, undirected star graphs $\mathcal{G}_{us}$, undirected cycle graphs $\mathcal{G}_{ucy}$, directed cycle graphs $\mathcal{G}_{dcy}$, and undirected regular ring lattices $\mathcal{G}^k_{url}$. It should be noted that $\mathcal{G}^k_{url}$ are highly structured networks with nodes placed on a ring, each connecting to its $2k$ nearest neighbors. Here, we consider the regular ring lattice $\mathcal{G}^2_{url}$. The graphic representation of these networks is available in [33] and omitted here. The graph Laplacians of these graphs on n agents are shown in Table I.

A. Continuous-Time Multi-Agent Networks

We first compare the D2CO H_∞ performance and the D2O H_∞ performance of the continuous-time system (6)-(11) on the above graphs. In particular, the D2CO H_∞ performance represents the influence of disturbances on consensus and control effort together. The trajectories of D2CO H_∞ performance on various number of agents for the above networks are depicted as solid curves in Fig. 2, which are consistent with Theorem 1 and Corollary 1. Obviously, the D2CO H_∞ performance index is always larger than 1. By contrast, if we dismiss the influence of disturbances on control effort, the D2CO H_∞ performance indices reduce to the D2O H_∞ performance indices (16) and (17), where (17) has been derived in [20], [21]. The trajectories of the D2O H_∞ performance are exhibited as dash curves in Fig. 2. As we can see, for each graph, the D2O H_∞ performance index is not greater than the D2CO H_∞ performance index. On the other hand, as the size of network increases, the D2CO H_∞ performance index and the D2O H_∞ performance index on the complete graph monotonically decreases and approaches to 1 and 0, respectively. The D2CO H_∞ performance index and the D2O H_∞ performance index on the star graph are always equal to $\sqrt{2}$ and 1, respectively. Both the D2CO H_∞ performance

TABLE I: Normal graph Laplacians of several directed and undirected graphs.

Notation	Graph Laplacian
$\mathcal{G}_{uc}$	$L_{uc} = \begin{bmatrix} n-1 & -1 & \cdots & -1 \\ -1 & n-1 & \cdots & -1 \\ \vdots & \vdots & \ddots & \vdots \\ -1 & -1 & \cdots & n-1 \end{bmatrix}$
$\mathcal{G}_{up}$	$L_{up} = \begin{bmatrix} 1 & -1 & 0 & \cdots & 0 \\ -1 & 2 & -1 & \cdots & 0 \\ \vdots & \ddots & \ddots & \ddots & \vdots \\ 0 & \cdots & -1 & 2 & -1 \\ 0 & \cdots & 0 & -1 & 1 \end{bmatrix}$
$\mathcal{G}_{us}$	$L_{us} = \begin{bmatrix} 1 & 0 & \cdots & 0 & -1 \\ 0 & 1 & \cdots & 0 & -1 \\ \vdots & \vdots & \ddots & \vdots & \vdots \\ 0 & 0 & \cdots & 1 & -1 \\ -1 & -1 & \cdots & -1 & n-1 \end{bmatrix}$
$\mathcal{G}_{ucy}$	$L_{ucy} = \begin{bmatrix} 2 & -1 & 0 & \cdots & -1 \\ -1 & 2 & -1 & \cdots & 0 \\ \vdots & \ddots & \ddots & \ddots & \vdots \\ 0 & \cdots & -1 & 2 & -1 \\ -1 & \cdots & 0 & -1 & 2 \end{bmatrix}$
$\mathcal{G}_{dcy}$	$L_{dcy} = \begin{bmatrix} 1 & -1 & 0 & \cdots & 0 \\ 0 & 1 & -1 & \cdots & 0 \\ \vdots & \vdots & \ddots & \ddots & \vdots \\ 0 & 0 & \cdots & 1 & -1 \\ -1 & 0 & \cdots & 0 & 1 \end{bmatrix}$
$\mathcal{G}^2_{url}$	$L_{url} = \begin{bmatrix} 4 & -1 & -1 & 0 & \cdots & -1 & -1 \\ -1 & 4 & -1 & -1 & \cdots & 0 & -1 \\ -1 & -1 & 4 & -1 & \cdots & 0 & 0 \\ \vdots & \ddots & \ddots & \ddots & \ddots & \ddots & \vdots \\ 0 & 0 & \cdots & -1 & 4 & -1 & -1 \\ -1 & 0 & \cdots & -1 & -1 & 4 & -1 \\ -1 & -1 & \cdots & 0 & -1 & -1 & 4 \end{bmatrix}$

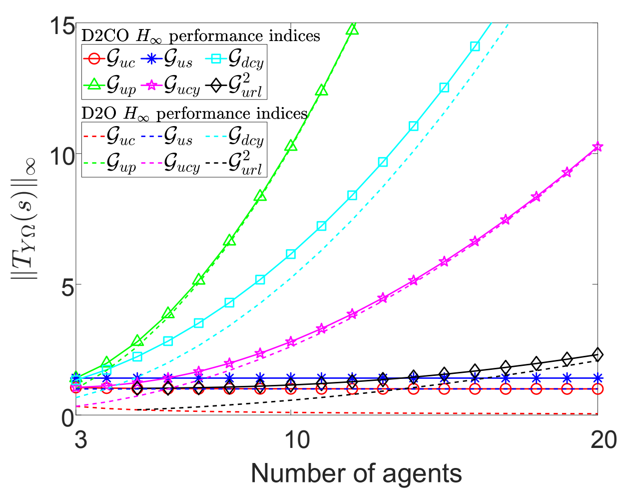

Fig. 2: Trajectories of the D2CO and the D2O H_∞ performance of the continuous-time multi-agent system (6)-(11).

index and the D2O H_∞ performance index on other graphs monotonically increases. In addition, either of the D2CO H_∞ performance and the D2O H_∞ performance on the complete graph is the best, and the path graph is the worst. Moreover, the undirected cycle graph outperforms its directed version all the time.

B. Sampled-Data Multi-Agent Networks

Then we explore the D2CO H_∞ performance and the optimal sampling period of the sampled-data multi-agent system (19)-(23) on aforementioned graphs. It is worth mentioning that Fig. 1 has uniformly depicted the trajectories of the D2CO H_∞ performance on any connected undirected graphs. Thus, we focus on the optimal sampling period on the above undirected graphs. In Fig. 3, the solid lines and the cycle-solid line display the trends of the upper bound of sampling period, i.e., $\frac{2}{\lambda_n}$, and the dash lines label the trends of the optimal sampling period h^*. It is observed from Fig. 3 that as the size of network increases, $\frac{2}{\lambda_n}$ of undirected graphs approaches to 0.5, 0.5, 0.32, 0 and 0, respectively. In addition, optimal sampling period h^* converges to $\frac{2}{\lambda_n}$ for each graph as the size of network increases. This means that the sampled-data multi-agent system (19)-(23) obtains the same H_∞ performance as the continuous-time multi-agent system (6)-(11) over almost the entire allowable range of sampling period if the scale of network topology is large enough. Combining Fig. 2 with Fig. 3, we can find that the sampled-data system (19)-(23) obtains better $\|T_{Y\Omega}(z)\|_\infty^*$ with smaller h^* among various undirected graphs. However, a small sampling period is difficult and extravagant in the applications. This interesting phenomenon illustrates the trade-off we need to make between robustness and sampling cost.

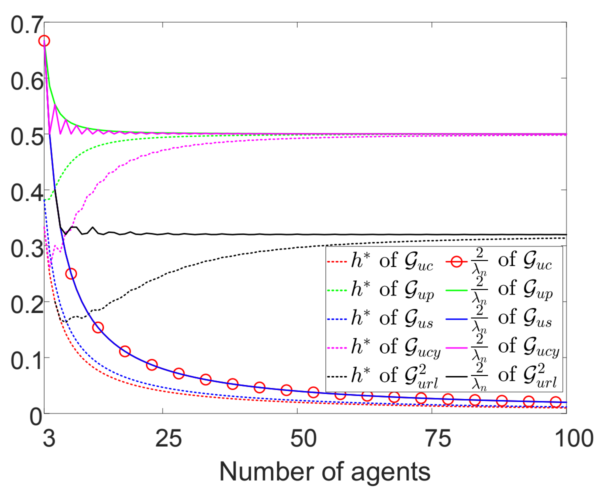

Fig. 3: Trends of h^* and $\frac{2}{\lambda_n}$ of the sampled-data multi-agent system (19)-(23) on various graphs.

On the other hand, most works [14]–[19] analyzed the H_∞ performance based on LMIs. However, they usually obtained numerical results. Furthermore, LMI technique is hard to reveal a quantitative relation between the H_∞ performance, the topological structure of the network and the sampling period like we show in (25). Therefore, we further compare our analytic result (25) of the D2CO H_∞ performance $\|T_{Y\Omega}(z)\|_\infty$ and its numerical result based on LMIs. In particular, we make the comparison on the well-known *small-world network* [38]. This network can be generated by randomly rewiring the regular ring lattice $\mathcal{G}_{url}^k$, which is widespread in real worlds such as power grids, social networks, and neural networks. Here, we randomly rewire the regular ring lattice $\mathcal{G}_{url}^2$ of 50 nodes with 0-1 edge weights and then obtain a small-world network denoted by $\mathcal{G}_{sw}^{50}$. The diagram of $\mathcal{G}_{sw}^{50}$ is shown in Fig. 4. Then, for different sampling periods, we invoke the *mincx solver* in Matlab Robust Control Toolbox and solve a series of LMIs to obtain approximate numerical estimations of $\|T_{Y\Omega}(z)\|_\infty$, where the LMIs are derived by applying the well-known *bounded-real lemma* [39] to the asymptotically stable subsystem (38). Here, the accuracy of the LMI solver is set to be 10^{-6}. Trajectories of the analytic result (25) and the numerical result of $\|T_{Y\Omega}(z)\|_\infty$ on various sampling periods are respectively depicted as the red solid curve and the blue dash curve in Fig. 5. It is obvious that the numerical result is basically consistent with our analytic result (25) within the preset tiny error 10^{-6}, and the optimal sampling period indeed exists and is unique. Moreover, combining Corollary 1 with Fig. 5, we can find that $\|T_{Y\Omega}(z)\|_\infty \geq \|T_{Y\Omega}(s)\|_\infty = 1.7674$, which is consistent with Corollary 3.

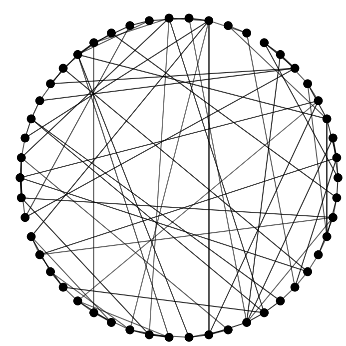

Fig. 4: Diagram of the small-world network $\mathcal{G}_{sw}^{50}$.

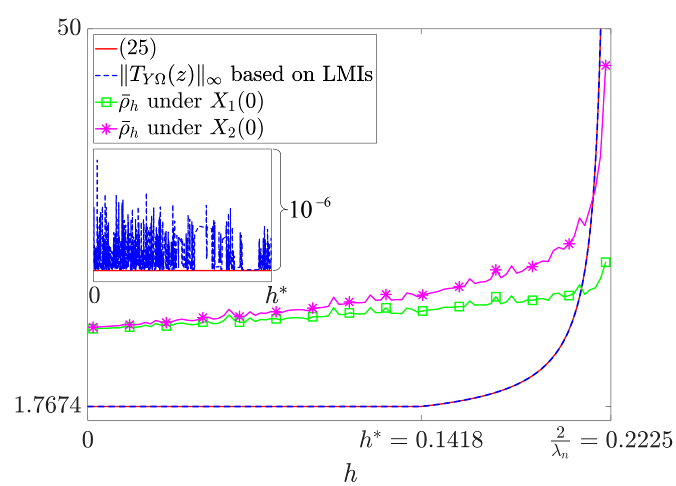

Fig. 5: Trajectories of the analytic result (25) and the numerical results of $\|T_{Y\Omega}(z)\|_\infty$ on various sampling period for $\mathcal{G}_{sw}^{50}$.

In the above tests, we only consider zero initial conditions, i.e., $X(0) = \mathbf{0}_n$. Here, we simulate the influence of non-zero initial conditions on the optimal sampling period for the small-world network $\mathcal{G}_{sw}^{50}$. Specifically, we approximately estimate the H_∞ performance index (22) over a finite set of sampled disturbances $\Pi = \{\Omega_i(t_k), t_k = kh, k \in \mathbb{N}\}_{i=1}^{N}$ instead of all disturbances in $\ell_2[0,\infty)$, where $N = 1000$, $\Omega_i(t_k) \in \mathbb{R}^{50}$ is periodically sampled from the continuous-time disturbance signal $\Omega_i(t) = [\Omega_i^1(t), \ldots, \Omega_i^{50}(t)]^\top \in \mathbb{R}^{50}$ by using a zero-order hold circuit with a sampling period $h > 0$, whose action time interval is only $[0, T]$ $(T = 10)$, and

$$\Omega_i^p(t) = \begin{cases} \cos(it)\sin[Tt - \cos(pi)t + i] & \text{if } p \text{ is odd}, \\ \sin(it)\cos[Tt + \sin(pi)t - i] & \text{if } p \text{ is even}, \\ p = 1, \ldots, 50. \end{cases}$$

Then, for any feasible sampling period, i.e., $0 < h < \frac{2}{\lambda_n} = 0.2225$, performance index (22) can be evaluated as

$$\bar{\rho}_h = \sup_{\Omega(t_k)\in\Pi} \sqrt{\frac{h\sum_{k=0}^{\infty}\left[e^\top(t_k)e(t_k) + U^\top(t_k)U(t_k)\right]}{h\sum_{k=0}^{\infty}\Omega^\top(t_k)\Omega(t_k)}}.$$

Here, we test two different non-zero initial conditions $X_1(0)$ and $X_2(0)$, where $X_1(0) = [1, \ldots, 50]^\top$ and each entry of $X_2(0)$ is randomly selected within $[-20, 20]$. The trajectories of $\bar{\rho}_h$ under $X_1(0)$ and $X_2(0)$ are portrayed as the square-solid curve and the star-solid curve in Fig. 5. It is shown that under non-zero initial conditions, the H_∞ performance is roughly a increasing function of the sampling period, that is, the optimal sampling period h^* no longer exists. However, these tests are only approximate estimations which need to be further theoretically analyzed in future works.

VI. Conclusion

In this paper, we analyzed the H_∞ performance of the first-order continuous-time multi-agent network and corresponding sampled-data multi-agent network against external disturbances, and revealed the relation between them. The H_∞ performance represents the influence of the disturbances on the quadratic performance index which contains both disagreement energy and control effort. Firstly, we built the relation between the H_∞ performance and the eigenvalues of Laplacian matrix for continuous-time multi-agent networks on directed and undirected graphs. Besides the properties of network topology, we elucidated how H_∞ performance depends on the sampling period for corresponding sampled-data multi-agent networks. We derived the optimal sampling period h^* such that the sampled-data multi-agent network obtains the optimal H_∞ performance. Furthermore, it was proved that periodic sampling cannot improve and at most maintain the H_∞ performance. We also proposed a simple sufficient condition for the optimal H_∞ performance problem, and a necessary and sufficient condition for the prescribed H_∞ performance problem. Finally, we used some numerical tests to illustrate our results. It was shown that the sampled-data network obtained better $\|T_{Y\Omega}(z)\|_\infty^*$ with smaller h^* among various undirected graphs. Whether the trade-off still exists for all connected undirected graphs is an interesting topic in future works.

Appendix

A. Proof of Theorem 1

Proof: The proof is divided into three main steps.

Step I: Obtaining the observable subsystem of system (6)-(11).

Since $\mathcal{G}$ has a spanning tree and L is normal, it follows from Lemma 2 that there exists an orthogonal matrix $Q = \begin{bmatrix} Q_1 & Q_2 \end{bmatrix} \in \mathbb{R}^{n\times n}$ $(Q_2 = \frac{\mathbf{1}_n}{\sqrt{n}})$ such that

$$Q^\top \Phi_n Q = \bar{\Phi}_n = \begin{bmatrix} I_{n-1} & \mathbf{0}_{n-1} \\ \mathbf{0}_{n-1}^\top & 0 \end{bmatrix} \tag{35}$$

and

$$Q^\top L Q = \bar{L} = \begin{bmatrix} \bar{L}_1 & \mathbf{0}_{n-1} \\ \mathbf{0}_{n-1}^\top & 0 \end{bmatrix}, \tag{36}$$

where $\bar{L}_1 \in \mathbb{R}^{(n-1)\times(n-1)}$ is also normal and has the same non-zero eigenvalues as L. Then performing the following orthogonal transformation

$$\hat{X}(t) = Q^\top X(t), \hat{\Omega}(t) = Q^\top \Omega(t), \hat{Y}(t) = \begin{bmatrix} Q^\top & \mathbf{0} \\ \mathbf{0} & Q^\top \end{bmatrix} Y(t),$$

for system (6)-(11) yields

$$\begin{cases} \dot{\hat{X}}(t) = -\bar{L}\hat{X}(t) + \hat{\Omega}(t), \\ \hat{Y}(t) = \begin{bmatrix} \bar{\Phi}_n \\ -\bar{L} \end{bmatrix} \hat{X}(t). \end{cases} \tag{37}$$

According to Lemma 1, L has a simple zero eigenvalue and all the other non-zero eigenvalues have positive real parts. Thus, $-\bar{L}_1$ is Hurwitz stable. In other words, system (37) can be divided into an asymptotically stable subsystem of order $n-1$ and a marginally stable subsystem of order 1. Clearly, the former is observable and determines the H_∞ performance, while the latter is unobservable and has no contribution to H_∞ performance. We turn to analyze the asymptotically stable subsystem

$$\begin{cases} \dot{\hat{X}}^1(t) = -\bar{L}_1\hat{X}^1(t) + \hat{\Omega}^1(t), \\ \hat{Y}^1(t) = \begin{bmatrix} I_{n-1} \\ -\bar{L}_1 \end{bmatrix} \hat{X}^1(t), \end{cases} \tag{38}$$

where $\hat{X}^1(t) = \begin{bmatrix} I_{n-1} & \mathbf{0}_{n-1} \end{bmatrix} \hat{X}(t)$ and $\hat{\Omega}^1(t) = \begin{bmatrix} I_{n-1} & \mathbf{0}_{n-1} \end{bmatrix} \hat{\Omega}(t)$. Let the transfer matrices of systems (37) and (38) be $T_{c1}(s)$ and $T_{c2}(s)$, respectively. Since $\bar{L}_1$ is normal, according to the spectral theorem [40], there exists a unitary matrix $V \in \mathbb{C}^{(n-1)\times(n-1)}$ such that

$$V^H \bar{L}_1 V = \Lambda, \tag{39}$$

where $\Lambda = \mathrm{diag}\{\lambda_2, \lambda_3, \ldots, \lambda_n\}$ consists of non-zero eigenvalues of L. Based on this property, $T_{c2}(s)$ can be rewritten as

$$T_{c2}(s) = \begin{bmatrix} V & \mathbf{0} \\ \mathbf{0} & V \end{bmatrix} \underbrace{\begin{bmatrix} (sI_{n-1} + \Lambda)^{-1} \\ -\Lambda(sI_{n-1} + \Lambda)^{-1} \end{bmatrix}}_{T_{c3}(s)} V^H. \tag{40}$$

Step II: Verifying that $\|T_{Y\Omega}(s)\|_\infty = \|T_{c3}(s)\|_\infty$.

It follows from

$$T_{c1}(s)=\begin{bmatrix}Q^\top & \mathbf{0}\\ \mathbf{0} & Q^\top\end{bmatrix}T_{Y\Omega}(s)Q=\begin{bmatrix}(sI_{n-1}+\bar{L}_1)^{-1} & \mathbf{0}_{n-1}\\ \mathbf{0}_{n-1}^\top & 0\\ -\bar{L}_1(sI_{n-1}+\bar{L}_1)^{-1} & \mathbf{0}_{n-1}\\ \mathbf{0}_{n-1}^\top & 0\end{bmatrix}$$

and

$$T_{c2}(s)=\begin{bmatrix}V & \mathbf{0}\\ \mathbf{0} & V\end{bmatrix}T_{c3}(s)V^H=\begin{bmatrix}(sI_{n-1}+\bar{L}_1)^{-1}\\ -\bar{L}_1(sI_{n-1}+\bar{L}_1)^{-1}\end{bmatrix}$$

that

$$T_{c1}^H(\mathbf{j}v)T_{c1}(\mathbf{j}v)=Q^\top T_{Y\Omega}^H(\mathbf{j}v)T_{Y\Omega}(\mathbf{j}v)Q,$$
$$T_{c2}^H(\mathbf{j}v)T_{c2}(\mathbf{j}v)=VT_{c3}^H(\mathbf{j}v)T_{c3}(\mathbf{j}v)V^H,$$
$$T_{c1}^H(\mathbf{j}v)T_{c1}(\mathbf{j}v)=\begin{bmatrix}T_{c2}^H(\mathbf{j}v)T_{c2}(\mathbf{j}v) & \mathbf{0}_{n-1}\\ \mathbf{0}_{n-1}^\top & 0\end{bmatrix}.$$

Then one can deduce that $\lambda_{max}[T_{Y\Omega}^H(\mathbf{j}v)T_{Y\Omega}(\mathbf{j}v)] = \lambda_{max}[T_{c1}^H(\mathbf{j}v)T_{c1}(\mathbf{j}v)] = \lambda_{max}[T_{c2}^H(\mathbf{j}v)T_{c2}(\mathbf{j}v)] = \lambda_{max}[T_{c3}^H(\mathbf{j}v)T_{c3}(\mathbf{j}v)]$. Therefore, according to the definition of H_∞ norm given in Property 2, we can obtain $\|T_{Y\Omega}(s)\|_\infty = \|T_{c1}(s)\|_\infty = \|T_{c2}(s)\|_\infty = \|T_{c3}(s)\|_\infty$. To sum up, computing $\|T_{Y\Omega}(s)\|_\infty$ can be converted to compute $\|T_{c3}(s)\|_\infty$.

Step III: Computing $\|T_{c3}(s)\|_\infty$ and obtaining its lower bound.

We can verify that $T_{c3}^H(\mathbf{j}v)T_{c3}(\mathbf{j}v) = \text{diag}\{\Upsilon_2,\dots,\Upsilon_n\}$, where

$$\Upsilon_i=\frac{1+|\lambda_i|^2}{Re^2(\lambda_i)+[Im(\lambda_i)+v]^2},\ i=2,\dots,n,\ v\in\mathbb{R}.$$

Note that $\sup_{v\in\mathbb{R}}\Upsilon_i=\frac{1+|\lambda_i|^2}{Re^2(\lambda_i)},\ i=2,\dots,n$. Therefore, we can obtain

$$\begin{aligned}\|T_{Y\Omega}(s)\|_\infty&=\|T_{c3}(s)\|_\infty\\&=\sup_{v\in\mathbb{R}}\sqrt{\lambda_{max}[T_{c3}^H(\mathbf{j}v)T_{c3}(\mathbf{j}v)]}\\&=\max_{i=2,\dots,n}\sqrt{\sup_{v\in\mathbb{R}}\Upsilon_i}\\&=\max_{i=2,\dots,n}\sqrt{\frac{1+|\lambda_i|^2}{Re^2(\lambda_i)}}.\end{aligned}$$

Apparently, $|\lambda_i|\geq Re(\lambda_i)$, $i=2,\dots,n$ and $0<Re(\lambda_2)\leq\dots\leq Re(\lambda_n)$ give rise to

$$\max_{i=2,\dots,n}\sqrt{\frac{1+|\lambda_i|^2}{Re^2(\lambda_i)}}\geq\sqrt{\frac{1+Re^2(\lambda_n)}{Re^2(\lambda_n)}}>1.$$

The proof is completed. ■

B. Proof of Theorem 2

Proof: The proof is divided into four main steps.

Step I: Obtaining the observable subsystem of system (19)-(23).

Note that $\mathcal{G}$ has a spanning tree and L is normal. It follows from Lemma 2 that there exists an orthogonal matrix $Q=\begin{bmatrix}Q_1 & Q_2\end{bmatrix}\in\mathbb{R}^{n\times n}$ ($Q_2=\frac{\mathbf{1}_n}{\sqrt{n}}$) such that (35) and (36) hold. Then we apply the following orthogonal transformation

$$\hat{X}(t_k)=Q^\top X(t_k),\hat{\Omega}(t_k)=Q^\top\Omega(t_k),\hat{y}(t_k)=\begin{bmatrix}Q^\top & \mathbf{0}\\ \mathbf{0} & Q^\top\end{bmatrix}y(t_k),$$

to system (19)-(23). Therefore, we have

$$\begin{cases}\hat{X}(t_{k+1})=P\hat{X}(t_k)+h\hat{\Omega}(t_k),\\ \hat{y}(t_k)=\begin{bmatrix}\bar{\Phi}_n\\ -\bar{L}\end{bmatrix}\hat{X}(t_k),\end{cases}\tag{41}$$

where

$$P=I_n-h\bar{L}=\begin{bmatrix}I_{n-1}-h\bar{L}_1 & \mathbf{0}_{n-1}\\ \mathbf{0}_{n-1}^\top & 1\end{bmatrix}$$

and $\bar{L}_1\in\mathbb{R}^{(n-1)\times(n-1)}$ is also normal which has the same non-zero eigenvalues as L. Since $0<h<\min_{i=2,\dots,n}\frac{2Re(\lambda_i)}{|\lambda_i|^2}$, the eigenvalues of $I_{n-1}-h\bar{L}_1$ satisfy $|\mu_i|=|1-h\lambda_i|<1$, $i=2,\dots,n$. Thus, $I_{n-1}-h\bar{L}_1$ is Schur stable. That is to say, system (19)-(23) can be decomposed into an asymptotically stable subsystem of order $n-1$ and a marginally stable subsystem of order 1. Obviously, the former determines the H_∞ performance, while the latter is unobservable and has no impact on H_∞ performance. Consider the asymptotically stable subsystem

$$\begin{cases}\hat{X}^1(t_{k+1})=(I_{n-1}-h\bar{L}_1)\hat{X}^1(t_k)+h\hat{\Omega}^1(t_k),\\ \hat{Y}^1(t_k)=\begin{bmatrix}I_{n-1}\\ -\bar{L}_1\end{bmatrix}\hat{X}^1(t_k),\end{cases}\tag{42}$$

where $\hat{X}^1(t_k)=\begin{bmatrix}I_{n-1} & \mathbf{0}_{n-1}\end{bmatrix}\hat{X}(t_k)$ and $\hat{\Omega}^1(t_k)=\begin{bmatrix}I_{n-1} & \mathbf{0}_{n-1}\end{bmatrix}\hat{\Omega}(t_k)$. Let the transfer matrices of systems (41) and (42) be $T_{d1}(z)$ and $T_{d2}(z)$, respectively. Since $\bar{L}_1$ is normal, (39) can be leveraged to decompose $T_{d2}(z)$ into

$$T_{d2}(z)=\begin{bmatrix}V & \mathbf{0}\\ \mathbf{0} & V\end{bmatrix}\underbrace{\begin{bmatrix}h(zI_{n-1}-I_{n-1}+h\Lambda)^{-1}\\ -h\Lambda(zI_{n-1}-I_{n-1}+h\Lambda)^{-1}\end{bmatrix}}_{T_{d3}(z)}V^H,$$

where $\Lambda=\text{diag}\{\lambda_2,\lambda_3,\dots,\lambda_n\}$ consists of non-zero eigenvalues of L.

Step II: Verifying that $\|T_{Y\Omega}(z)\|_\infty=\|T_{d3}(z)\|_\infty$.

It follows from

$$\begin{aligned}T_{d1}(z)&=\begin{bmatrix}Q^\top & \mathbf{0}\\ \mathbf{0} & Q^\top\end{bmatrix}T_{Y\Omega}(z)Q\\&=\begin{bmatrix}h(zI_{n-1}-I_{n-1}+h\bar{L}_1)^{-1} & \mathbf{0}_{n-1}\\ \mathbf{0}_{n-1}^\top & 0\\ -h\bar{L}_1(zI_{n-1}-I_{n-1}+h\bar{L}_1)^{-1} & \mathbf{0}_{n-1}\\ \mathbf{0}_{n-1}^\top & 0\end{bmatrix}\end{aligned}$$

and

$$\begin{aligned}T_{d2}(z)&=\begin{bmatrix}V & \mathbf{0}\\ \mathbf{0} & V\end{bmatrix}T_{d3}(z)V^H\\&=\begin{bmatrix}h(zI_{n-1}-I_{n-1}+h\bar{L}_1)^{-1}\\ -h\bar{L}_1(zI_{n-1}-I_{n-1}+h\bar{L}_1)^{-1}\end{bmatrix}\end{aligned}$$

that

$$T_{d1}^H(\mathrm{e}^{\mathbf{j}v})T_{d1}(\mathrm{e}^{\mathbf{j}v})=Q^\top T_{Y\Omega}^H(\mathrm{e}^{\mathbf{j}v})T_{Y\Omega}(\mathrm{e}^{\mathbf{j}v})Q,$$
$$T_{d2}^H(\mathrm{e}^{\mathbf{j}v})T_{d2}(\mathrm{e}^{\mathbf{j}v})=VT_{d3}^H(\mathrm{e}^{\mathbf{j}v})T_{d3}(\mathrm{e}^{\mathbf{j}v})V^H,$$
$$T_{d1}^H(\mathrm{e}^{\mathbf{j}v})T_{d1}(\mathrm{e}^{\mathbf{j}v})=\begin{bmatrix}T_{d2}^H(\mathrm{e}^{\mathbf{j}v})T_{d2}(\mathrm{e}^{\mathbf{j}v}) & \mathbf{0}_{n-1}\\ \mathbf{0}_{n-1}^\top & 0\end{bmatrix}.$$

Then we can deduce that $\lambda_{max}[T_{Y\Omega}^H(\mathrm{e}^{\mathbf{j}v})T_{Y\Omega}(\mathrm{e}^{\mathbf{j}v})] = \lambda_{max}[T_{d1}^H(\mathrm{e}^{\mathbf{j}v})T_{d1}(\mathrm{e}^{\mathbf{j}v})] = \lambda_{max}[T_{d2}^H(\mathrm{e}^{\mathbf{j}v})T_{d2}(\mathrm{e}^{\mathbf{j}v})] =$

$\lambda_{max}[T_{d3}^H(e^{\mathbf{j}v})T_{d3}(e^{\mathbf{j}v})]$. Therefore, according to the definition of H_∞ norm given in Property 4, we can get $\|T_{Y\Omega}(z)\|_\infty = \|T_{d1}(z)\|_\infty = \|T_{d2}(z)\|_\infty = \|T_{d3}(z)\|_\infty$. Compared with $\|T_{Y\Omega}(z)\|_\infty$, $\|T_{d3}(z)\|_\infty$ is more computationally tractable.

Step III: Turning to calculate $\|T_{d3}(z)\|_\infty$.

Noticing the fact $e^{\mathbf{j}v} = \cos v + \mathbf{j}\sin v$, we can verify that $T_{d3}^H(e^{\mathbf{j}v})T_{d3}(e^{\mathbf{j}v}) = \mathrm{diag}\{\Psi_2, \ldots, \Psi_n\}$, where

$$\begin{aligned}\Psi_i &= \frac{h^2 + h^2|\lambda_i|^2}{\big[\cos v + hRe(\lambda_i) - 1\big]^2 + \big[\sin v + hIm(\lambda_i)\big]^2} \\ &= \frac{h^2 + h^2|\lambda_i|^2}{1 + |\mu_i|^2 + 2hIm(\lambda_i)\sin v + 2\big[hRe(\lambda_i) - 1\big]\cos v} \\ &= \frac{h^2 + h^2|\lambda_i|^2}{1 + |\mu_i|^2 + 2|\mu_i| f_i(v)},\end{aligned}$$

$i = 2, \ldots, n$, $v \in [0, 2\pi]$ and

$$f_i(v) = \begin{cases} \sin\Big(v + \arctan\dfrac{hRe(\lambda_i) - 1}{hIm(\lambda_i)}\Big) \\ \text{if } Im(\lambda_i) > 0, \\ \cos\Big(v - \arctan\dfrac{hIm(\lambda_i)}{hRe(\lambda_i) - 1}\Big) \\ \text{if } \dfrac{1}{h} < Re(\lambda_i), \\ \sin\Big(v + \pi + \arctan\dfrac{hRe(\lambda_i) - 1}{hIm(\lambda_i)}\Big) \\ \text{if } Im(\lambda_i) \le 0,\ 0 < Re(\lambda_i) \le \dfrac{1}{h}. \end{cases}$$

It follows from $-1 \le f_i(v) \le 1$ that

$$\begin{aligned}\sup_{v\in[0,2\pi]} \Psi_i &= \frac{h^2 + h^2|\lambda_i|^2}{1 + |\mu_i|^2 - 2|\mu_i|} \\ &= \frac{h^2 + h^2|\lambda_i|^2}{(1 - |\mu_i|)^2},\ i = 2, \ldots, n.\end{aligned}$$

Thus, one can obtain

$$\begin{aligned}\|T_{Y\Omega}(z)\|_\infty = \|T_{d3}(z)\|_\infty &= \sup_{v\in[0,2\pi]} \sqrt{\lambda_{max}[T_{d3}^H(e^{\mathbf{j}v})T_{d3}(e^{\mathbf{j}v})]} \\ &= \max_{i=2,\ldots,n} \sqrt{\sup_{v\in[0,2\pi]} \Psi_i} \\ &= \max_{i=2,\ldots,n} h\sqrt{\frac{1 + |\lambda_i|^2}{(1 - |\mu_i|)^2}}.\end{aligned}$$

Step IV: Deriving the lower bound of $\|T_{Y\Omega}(z)\|_\infty$.

Furthermore, it follows from $1 + |\lambda_i|^2 \ge 1 + Re^2(\lambda_i)$ and $1 - |\mu_i| \le 1 - |1 - hRe(\lambda_i)|$ that

$$\begin{aligned} h\sqrt{\frac{1 + |\lambda_i|^2}{(1 - |\mu_i|)^2}} &\ge h\sqrt{\frac{1 + Re^2(\lambda_i)}{(1 - |1 - hRe(\lambda_i)|)^2}} \\ &= \begin{cases} \sqrt{\dfrac{1 + Re^2(\lambda_i)}{Re^2(\lambda_i)}} & 0 < h \le \dfrac{1}{Re(\lambda_i)}, \\ h\sqrt{\dfrac{1 + Re^2(\lambda_i)}{(2 - hRe(\lambda_i))^2}} & \dfrac{1}{Re(\lambda_i)} \le h < \dfrac{2}{Re(\lambda_i)}, \end{cases} \\ &\ge \sqrt{1 + \frac{1}{Re^2(\lambda_i)}} > 1,\ \forall h \in \Big(0, \frac{2}{Re(\lambda_i)}\Big),\end{aligned}$$

for $i = 2, \ldots, n$. Since $\frac{2Re(\lambda_i)}{|\lambda_i|^2} \le \frac{2}{Re(\lambda_i)}$, we can get $\min\limits_{i=2,\ldots,n} \frac{2Re(\lambda_i)}{|\lambda_i|^2} \le \frac{2}{Re(\lambda_i)}$, $\forall i \in \{2, \ldots, n\}$. Therefore, we can obtain

$$h\sqrt{\frac{1 + |\lambda_i|^2}{(1 - |\mu_i|)^2}} > 1,\ \forall h \in \Big(0, \min_{i=2,\ldots,n} \frac{2Re(\lambda_i)}{|\lambda_i|^2}\Big)$$

for any $i = 2, \ldots, n$. Then it can be notably concluded that

$$\max_{i=2,\ldots,n} h\sqrt{\frac{1 + |\lambda_i|^2}{(1 - |\mu_i|)^2}} > 1.$$

The proof is completed. ■

References

[1] A. Jadbabaie, J. Lin, and A. S. Morse, "Coordination of groups of mobile autonomous agents using nearest neighbor rules," *IEEE Transactions on Automatic Control*, vol. 48, no. 6, pp. 988–1001, 2003.

[2] T. Vicsek, A. Czirók, E. Ben-Jacob, I. Cohen, and O. Shochet, "Novel type of phase transition in a system of self-driven particles," *Physical Review Letters*, vol. 75, no. 6, pp. 1226–1229, 1995.

[3] R. Olfati-Saber, J. A. Fax, and R. M. Murray, "Consensus and cooperation in networked multi-agent systems," *Proceedings of the IEEE*, vol. 95, no. 1, pp. 215–233, 2007.

[4] W. Ren and R. W. Beard, "Consensus seeking in multiagent systems under dynamically changing interaction topologies," *IEEE Transactions on Automatic Control*, vol. 50, no. 5, pp. 655–661, 2005.

[5] Y. Zheng, Y. Zhu, and L. Wang, "Consensus of heterogeneous multi-agent systems," *IET Control Theory & Applications*, vol. 5, no. 16, pp. 1881–1888, 2011.

[6] Q. Zhao, Y. Zheng, J. Ma, and S. Chen, "Winner-take-all competition with heterogeneous dynamic agents," *Neurocomputing*, vol. 374, pp. 42–48, 2020.

[7] Y. Zheng, J. Ma, and L. Wang, "Consensus of hybrid multi-agent systems," *IEEE Transactions on Neural Networks and Learning Systems*, vol. 29, no. 4, pp. 1359–1365, 2018.

[8] Q. Zhao, Y. Zheng, J. Liu, and B. Liu, "Further analysis for consensus of hybrid multiagent systems: A unified framework," *International Journal of Robust and Nonlinear Control*, vol. 31, no. 16, pp. 8109–8117, 2021.

[9] L. Zhou, J. Wang, M. Ye, B.-L. Zhang, and Y. Zheng, "Consensus of hybrid behavior for graphical coordination games," *IEEE Transactions on Circuits and Systems II: Express Briefs*, vol. 70, no. 8, pp. 3009–3013, 2023.

[10] L. Zhou, J. Liu, Y. Zheng, F. Xiao, and J. Xi, "Game-based consensus of hybrid multiagent systems," *IEEE Transactions on Cybernetics*, vol. 53, no. 8, pp. 5346–5357, 2023.

[11] G. F. Young, L. Scardovi, and N. E. Leonard, "Robustness of noisy consensus dynamics with directed communication," in *Proceedings of the 2010 American Control Conference*, 2010, pp. 6312–6317.

[12] H. G. Oral, E. Mallada, and D. F. Gayme, "Performance of first and second order linear networked systems over digraphs," in *Proceedings of the 2017 IEEE Conference on Decision and Control*, 2017, pp. 1688–1694.

[13] S. Dezfulian, Y. Ghaedsharaf, and N. Motee, "On performance of time-delay linear consensus networks with directed interconnection topologies," in *Proceedings of the 2018 American Control Conference*, 2018, pp. 4177–4182.

[14] P. Lin, Y. Jia, and L. Li, "Distributed robust H_∞ consensus control in directed networks of agents with time-delay," *Systems & Control Letters*, vol. 57, no. 8, pp. 643–653, 2008.

[15] Y. Liu and Y. Jia, "Consensus problem of high-order multi-agent systems with external disturbances: An H_∞ analysis approach," *International Journal of Robust and Nonlinear Control*, vol. 20, no. 14, pp. 1579–1593, 2010.

[16] Y. Liu and Y. Jia, "H_∞ consensus control for multi-agent systems with linear coupling dynamics and communication delays," *International Journal of Systems Science*, vol. 43, no. 1, pp. 50–62, 2012.

[17] Z. Li, Z. Duan, and G. Chen, "On H_∞ and H_2 performance regions of multi-agent systems," *Automatica*, vol. 47, no. 4, pp. 797–803, 2011.

[18] Y. Ao and Y. Jia, "Output feedback control of mixed H_2/H_∞ multi-agent consensus via an inner auxiliary system approach," *Systems & Control Letters*, vol. 158, p. 105064, 2021.

[19] A. Shams, M. Rehan, and M. Tufail, "H_∞ bipartite consensus of nonlinear multi-agent systems over a directed signed graph with a leader of non-zero input," *International Journal of Control*, vol. 95, no. 7, pp. 1944–1958, 2022.

[20] M. Pirani, E. M. Shahrivar, B. Fidan, and S. Sundaram, "Robustness of leader–follower networked dynamical systems," *IEEE Transactions on Control of Network Systems*, vol. 5, no. 4, pp. 1752–1763, 2018.

[21] M. Siami and N. Motee, "Systemic measures for performance and robustness of large-scale interconnected dynamical networks," in *Proceedings of the 2014 IEEE Conference on Decision and Control*, 2014, pp. 5119–5124.

[22] D. Zelazo and M. Mesbahi, "Edge agreement: Graph-theoretic performance bounds and passivity analysis," *IEEE Transactions on Automatic Control*, vol. 56, no. 3, pp. 544–555, 2011.

[23] J. Wang, L. Zhou, D. Zhang, J. Liu, and Y. Zheng, "Protocol selection for second-order consensus against disturbance," *arXiv preprint*, 2022, https://doi.org/10.48550/arXiv.2212.05240.

[24] M. Pirani, H. Sandberg, and K. H. Johansson, "A graph-theoretic approach to the H_∞ performance of leader–follower consensus on directed networks," *IEEE Control Systems Letters*, vol. 3, no. 4, pp. 954–959, 2019.

[25] Y. Cao and W. Ren, "Optimal linear-consensus algorithms: An LQR perspective," *IEEE Transactions on Systems, Man, and Cybernetics, Part B (Cybernetics)*, vol. 40, no. 3, pp. 819–830, 2010.

[26] G. Xie, H. Liu, L. Wang, and Y. Jia, "Consensus in networked multi-agent systems via sampled control: Fixed topology case," in *Proceedings of the 2009 American Control Conference*, 2009, pp. 3902–3907.

[27] Y. Cao and W. Ren, "Multi-vehicle coordination for double-integrator dynamics under fixed undirected/directed interaction in a sampled-data setting," *International Journal of Robust and Nonlinear Control*, vol. 20, no. 9, pp. 987–1000, 2010.

[28] Y. Zheng and L. Wang, "Consensus of switched multiagent systems," *IEEE Transactions on Circuits and Systems II: Express Briefs*, vol. 63, no. 3, pp. 314–318, 2016.

[29] X. Ge, Q.-L. Han, D. Ding, X.-M. Zhang, and B. Ning, "A survey on recent advances in distributed sampled-data cooperative control of multi-agent systems," *Neurocomputing*, vol. 275, pp. 1684–1701, 2018.

[30] M. J. Corless and A. Frazho, *Linear Systems and Control: An Operator Perspective*. Marcel Dekker, Inc, 2003.

[31] X. Guo, J. Wang, F. Liao, and R. S. H. Teo, *Multi-Agent Systems: Platoon Control and Non-Fragile Quantized Consensus*. CRC Press, 2019.

[32] B. M. Chen, *Robust and H_∞ Control*. Springer-Verlag London, 2000.

[33] F. L. Lewis, H. Zhang, K. Hengster-Movric, and A. Das, *Cooperative Control of Multi-Agent Systems: Optimal and Adaptive Design Approaches*. Springer-Verlag London, 2014, ch. 2, pp. 23–71.

[34] M. Siami and N. Motee, "Network sparsification with guaranteed systemic performance measures," *IFAC-PapersOnLine*, vol. 48, no. 22, pp. 246–251, 2015.

[35] J. Wang, Z. Duan, Y. Zhao, G. Qin, and Y. Yan, "H_∞ and H_2 control of multi-agent systems with transient performance improvement," *International Journal of Control*, vol. 86, no. 12, pp. 2131–2145, 2013.

[36] T. Li and J.-F. Zhang, "Mean square average-consensus under measurement noises and fixed topologies: Necessary and sufficient conditions," *Automatica*, vol. 45, no. 8, pp. 1929–1936, 2009.

[37] C. Godsil and G. F. Royle, *Algebraic Graph Theory*. Springer-Verlag New York, 2001.

[38] D. J. Watts and S. H. Strogatz, "Collective dynamics of 'small-world' networks," *Nature*, vol. 393, pp. 440–442, 1998.

[39] L. Yu, *Robust Control: LMI Approach*. Beijing: Tsinghua University Press, 2022, (in Chinese).

[40] R. A. Horn and C. R. Johnson, *Matrix Analysis*. Cambridge University Press, 2012.

Jiamin Wang was born in Yinchuan, China. He received the B.S. degree from Chang'an University in 2019. He is currently working toward the Ph.D. degree in complex systems at Xidian University. His research interests are currently focused on robust control, multi-agent systems, complex networks, and collective intelligence.

Jian Liu received the B.S. degree in mathematics from Fuyang Normal University, Fuyang, China, in 2007, the M.S. degree in mathematics from Donghua University, Shanghai, China, in 2010, and the Ph.D. degree in mathematics from Xi'an Jiaotong University, Xi'an, China, in 2017. Since 2017, he has been with the Center for Complex Systems, School of Mechano-Electronic Engineering, Xidian University, Xi'an. His research interests include iterative learning control, networked control systems, and complex networks.

Yuanshi Zheng (Senior Member, IEEE) was born in Jiangshan, China. He received the B.S. and M.S. degrees in applied mathematics from Ningxia University, Yinchuan, China, in 2006 and 2009, respectively, and the Ph.D. degree from Xidian University, Xi'an, China, in 2012. He is currently a Professor with Xidian University. His research interests include coordination of multi-agent systems, game theory, and collective intelligence.

Jianxiang Xi received the B.S. and M.S. degrees in High-Tech Institute of Xi'an, China in 2004 and 2007, respectively. He received the Ph.D. degree in control science and engineering from Rocket Force University of Engineering, Xi'an, China in 2012 by a coalition form with Tsinghua University. He is currently a professor in control science and engineering of Rocket Force University of Engineering. His research interests include complex systems control, switched systems, and swarm systems.